MINISTÉRIO DA EDUCAÇÃO
UNIVERSIDADE FEDERAL RURAL DA AMAZÔNIA
PROGRAMA DE PÓS-GRADUAÇÃO EM AGRONOMIA

BRENO RICARDO SERRÃO DA SILVA

STRUCTURAL, BIOCHEMICAL, PHYSIOLOGICAL AND NUTRITIONAL RESPONSES IN SOYBEAN PLANTS UNDER PROGRESSIVE SALT STRESS

BELÉM-PA
2020

BRENO RICARDO SERRÃO DA SILVA

STRUCTURAL, BIOCHEMICAL, PHYSIOLOGICAL AND NUTRITIONAL RESPONSES IN SOYBEAN PLANTS UNDER PROGRESSIVE SALT STRESS

Thesis submitted to Universidade Federal Rural da Amazônia, as part of the requirements for obtaining the *Doctor Scientiae* degree in Agronomy.
Concentration area: Agronomy.
Advisor: Prof. Dr. Allan Klynger da Silva Lobato

BELÉM-PA

2020

BRENO RICARDO SERRÃO DA SILVA

STRUCTURAL, BIOCHEMICAL, PHYSIOLOGICAL AND NUTRITIONAL RESPONSES IN SOYBEAN PLANTS UNDER PROGRESSIVE SALT STRESS

Thesis submitted to Universidade Federal Rural da Amazônia, as part of the requirements for obtaining the *Doctor Scientiae* degree in Agronomy.
Concentration area: Agronomy.
Advisor: Dr. Allan Klynger da Silva Lobato

_____/_____/_____
Approval date

EXAMINATION BOARD

_____
Prof. Dr. Allan Klynger da Silva Lobato – Advisor
UNIVERSIDADE FEDERAL RURAL DA AMAZÔNIA – UFRA

_____
Prof. Dr. Flávio José Rodrigues Cruz – 1st Examiner
UNIVERSIDADE FEDERAL RURAL DE PERNAMBUCO – UFRPE

_____
Prof. Dra. Rafaela Cabral dos Santos da Trindade – 2nd Examiner

_____
Prof. Dr. Marco Antônio Menezes Neto – 3rd Examiner
UNIVERSIDADE FEDERAL DO PARÁ – UFPA

_____
Prof. Dr. Seidel Ferreira dos Santos – 4rd Examiner
UNIVERSIDADE ESTADUAL DO PARÁ – UEPA

_____
Prof. Dr. João Rodrigo Coimbra Nobre – Alternate Examiner
UNIVERSIDADE ESTADUAL DO PARÁ – UEPA

To my parents, ***Luziel Santos*** *and* ***Socorro Serrão****; my brother* ***Luziel Júnior****; my goddaughter* ***Sofia Serrão*** *who offered a lot of affection, support and were important to reach this stage of my life.*

I DEDICATED

ACKNOWLEDGEMENTS

The **Universidade Federal Rural da Amazônia (UFRA)** and **Museu Paraense Emílio Goeldi (MPEG)** for the formation and infrastructure provided;

The **Coordenação de Aperfeiçoamento de Pessoal de Nível Superior (CAPES)** for granting the scholarship;

To **Dr. Allan Klynger da Silva Lobato** for his orientation, patience and all the support provided for my formation;

To the **examining board** for having accepted the invitation and given to contribute to the thesis;

To the **professors of the postgraduate course** and **associates** for the subjects taught, discussions and teachings;

To **all users of the Laboratório de Anatomia Vegetal** (LAVEG) and the **Núcleo de Pesquisa Vegetal Básica e Aplicada (NPVBA)** for the exchange of information and pleasure moments that made the work environment a pleasant and mutually supportive place;

To **Dra. Alba Lins** for the valuable lessons throughout this period that I was at LAVEG, for the words of encouragement and contributions in the laboratory;

My **family**, especially my parents **Luziel Santos** and **Socorro Serrão** for their education; my brother **Luziel Júnior**, always serving as inspiration for my aim; and my goddaughter **Sofia Serrão**, who, although very young, provided moments of joy which were fundamental for the renewal of strength and forging ahead;

To **all my friends** who made everything more fun and unforgettable moments

And to everyone who directly or indirectly took part in the realization of my dream.

Thank you!

RESUMO

A soja é uma leguminosa largamente cultivada em diversos países devido aos elevados teores de proteínas e óleos contidos em seus grãos. É utilizada na alimentação humana e animal ou destinada a produção de medicamentos, produtos industriais e biocombustível. Por outro lado, o estresse salino é um fator limitante na produção da cultura e estima-se que mais de 800 milhões de hectares são afetadas pela salinidade. Nesse sentido, o objetivo dessa pesquisa foi avaliar o comportamento estrutural, utilizando variáveis da raíz, caule e folha, detalhando as possíveis modificações anatômicas envolvidas nesses órgãos, além de compreender o comportamento nutricional, o aparato fotossintético, trocas gasosas, sistema antioxidante e danos oxidativo em plantas de soja submetidas a estresse salino progressivo. Para isso, o experimento foi randomizado em cinco tratamentos (0, 50, 100, 150 e 200 mM de NaCl). Na raíz, aumentos na epiderme e endoderme revelam os papeis protetores dessas estruturas em plantas submetidas até 100 mM Na^+, que favorecem a redução do influxo de Na^+. Com o incremento da salinidade, o maior aumento do aerênquima lisígeno minimiza a absorção de íon tóxicos através da substituição das células mortas por espaços de ar. Em relação ao caule, aumentos no córtex e na medula, no primeiro entrenó nas concentrações de 100 mM Na^+, amenizam os danos e estresse oxidativo gerados pelo sal nas regiões meristemáticas. Em todas as regiões da raiz e do caule analisadas nas plantas de soja submetidas a concentrações de 50-200 mM Na^+, o metaxilema é reduzido para evitar a cavitação e perda da funcionalidade dos elementos de vasos e, essas alterações, maximiza a impermeabilidade deste tecido evitando o fluxo iônico através do aumento da espessura da parede celular. Em relação às folhas, o estresse salino progressivo interfere negativamente na homeostase de K^+/Na^+, o conteúdo nutricional, aparato fotossintético e trocas gasosas, também aumenta o dano oxidativo e, em certa medida, induz o sistema antioxidante e prejudica os pigmentos fotossintéticos. Por outro lado, os impactos da salinidade promovem modificações anatômicas foliares que minimizam os efeitos deletérios associados ao Na^+. Efeitos como o aumento da cera epicuticular em concentrações salinas de 50 mM Na^+ favorecem uma proteção lipofílica que evita a perda de água pela transpiração e a incidência direta da radiação solar nas células epidérmicas. Além disso, as melhorias observadas na quantidade dos estômatos, em sua forma mais elíptica, bem como o aumento da espessura da epiderme, até 100 mM Na^+, evidenciam uma estratégia para o uso eficiente da água. Por fim, esta pesquisa mostrou que plantas de soja submetidas a estresse salino progressivo exibiram modificações anatômicas para minimizar os efeitos deletérios associados ao Na^+.

Palavras-chave: Exclusão de Na^+, *Glycine max*, Salinidade, Sódio.

ABSTRACT

Soybean is a legume that is widely cultivated in many countries due to the high levels of proteins and oils contained in its grains. It is used in human and animal nutrition or for the production of medicines, industrial products and biofuel. On the other hand, salt stress is a limiting factor in crop production and it is estimated that more than 800 million hectares are affected by salinity. In this sense, the aim of this research was to evaluate the structural behavior, using root, stem and leaf variables, detailing the possible anatomical changes involved in these organs, in addition to understanding the nutritional behavior, the photosynthetic apparatus, gas exchange, antioxidant system and oxidative damage in soybean plants submitted to progressive salt stress. For this, the experiment was randomized into five treatments (0, 50, 100, 150 and 200 mM NaCl). In the root, increases in the epidermis and endoderm reveal the protective roles of these structures in plants subjected to 100 mM Na^+, which favor the reduction of the influx of Na^+. With the increase in salinity, the higher increase in the lysigenous aerenchyma minimizes the absorption of toxic ions by replacing dead cells with air spaces. In relation to the stem, increases in the cortex and pith, in the first internode in concentrations of 100 mM Na^+, alleviate the damage and oxidative stress generated by salt in the meristematic regions. In all root and stem regions analyzed in soybean plants subjected to concentrations of 50-200 mM Na^+, the metaxylem is reduced to prevent cavitation and loss of functionality of vessel elements and, these changes, maximizes the impermeability of this tissue preventing ionic flux by increase the thickness of the cell wall. In relation to leaves, progressive salt stress negatively interferes in K^+/Na^+ homeostasis, nutritional content, photosynthetic apparatus and gas exchange, also increases oxidative damage and, to some extent, induces the antioxidant system and harms photosynthetic pigments. On the other hand, the impacts of salinity promote leaf anatomical changes to minimize the deleterious effects associated with Na^+. Effects such the increase of epicuticular wax in saline concentrations of 50 mM Na^+ favor a lipophilic protection that prevents the loss of water through transpiration and the direct incidence of solar radiation in the epidermal cells. In addition, the improvements observed in the number of stomata, in their most elliptical form, as well as the increase in the thickness of the epidermis, up to 100 mM Na^+, evidence a strategy for the efficient use of water. Finally, this research showed that soybean plants subjected to progressive salt stress exhibited anatomical changes to minimize the deleterious effects associated with Na +.

Keywords: *Glycine max*, Na^+ exclusion, Salinity, Sodium.

SUMMARY

CONTEXTUALIZATION

Soybean [*Glycine max* (L.) Merr.], belonging to Fabaceae and Papilionoideae, is a species from China and adjacent regions (FREITAS, 2011), in which its improvement began with the appearance of plants from natural crossings, between two wild soybean species that have been domesticated and improved by scientists from ancient China (FARIAS et al., 2007; LEE et al., 2011). The records indicate that *G. max* was derived from *G. gracilis*, which in turn has *G. soy* as an ancestor (MISSION, 2006).

In Brazil, the first crop was registered in Bahia via the United States, in 1882, by Gustavo Dutra, then professor at the Bahia School of Agronomy, who conducted the first evaluation studies of cultivars introduced in the country (MUSSKOPF; BIER, 2010). In 1891, cultivar adaptation tests were performed at the Agronomic Institute of Campinas, State of São Paulo (SP). At that time, the interest was only forage use and its use as grain was only started in 1941 in Rio Grande do Sul (ROCHA, 2009).

Soybean is an annual, autogamous, herbaceous, erect plant with wide variability in morphological characteristics that can still be influenced by various environmental conditions (MATTOS et al., 2016). Its cycle, which is the number of days from emergence to maturity, can take from 75 days for the earliest cultivars and 200 days for the later ones (SEDIYAMA, 2009).

The root system is pivotal, with a main root and profuse lateral branches capable of establishing symbiosis with atmospheric nitrogen-fixing bacteria (NICOLOSO et al., 2008). The stem is hairy and often branched, with a height between 30 and 200 cm and can have indeterminate, semi-determined or determined growth (CAPELLARI JUNIOR et al., 2007).

Cultivars of undetermined growth do not have terminal flowering branches and continue to develop knots and lengthen the stem so that they continue to increase height until the end of flowering (ROCHA, 2009). While cultivars with a determined growth habit have plants with stems terminated by floral races and, after flowering begins, the plants increase very little in height (SOUZA et al., 2014).

The leaves are alternate, of long petioles and composed of three large, usually oval leaflets. The flowers are axillary or terminal, papillary type, white, yellow or violet, depending on the variety (BORÉM, 1999). The fruits are oblong and hanging pods, pubescent and 25 to 75 mm long, with grains numbering from one to five per vage (BORÉM, 2005). These are mostly elliptical and flat and in a state of maturity, they may have a straw yellow, olive, light brown or black color in the cultivated varieties (MISSÃO, 2006).

The soybean cycle is divided into developmental, vegetative and reproductive stages. The vegetative stages are named by the letter V and the reproductive stages by the letter R. With the exception of emergence and opening events of the cotyledons, the letters V and R are followed by numbers that identify specific stages (ROCHA, 2009). The V stages correspond to the events that occurred since the seedling emergence until the last trifoliate emission before the first flower opening. While the R stages comprise the events that occurred from the opening of the first flower to the complete maturation of the pods (FAGAN et al., 2010).

Currently, soybeans are cultivated in several countries due to the high levels of protein and oil contained in their grains (BRUNINI et al., 2016). It is used in human and animal food (RENNÓ, 2015; ZAKIR; FREITAS, 2015), or intended for the production of medicines, industrial products and biofuel (STACHIW et al., 2016). Given this global need, soybeans are an essential and growing crop for many productive sectors.

The USA leads the world soy production followed by Brazil (AGRIANUAL, 2016; FAO, 2019). In this country, production is predominantly concentrated in the Midwest and South regions, with Mato Grosso being the main producer of the crop. In the North, Pará deserves to be highlighted as the second largest producer in the region (IBGE, 2016).

The advance of soybean has been occurring in all regions of the country, especially in the North and Northeast (CONAB, 2016). However, the constant use of technologies such as excessive application of fertilizers, pesticides, irrigation water in productive environments can cause serious damage to the biosphere, one of them is salinization of soils (PEDROTTI et al., 2015).

Soil salinization is a growing problem worldwide. Approximately 800 million hectares of soils are estimated to be affected by salts (FAO, 2019), with most of the world's irrigated areas suffering from reduced yields due to excess salts in the soil (RIBEIRO et al., 2003; SOUSA , 2007). Salt-affected soils are mainly found in arid and semi-arid climates in more than 100 countries on all continents except Antarctica. In Brazil the problem is verified throughout the country, especially in the Northeast, where approximately 25% of irrigated areas were salinized (GHEYI, 2000).

Man-induced salinization is most noticeable in environments with high evapotranspiration and low rainfall throughout the year, manifesting itself most markedly in these areas due to inadequate irrigation management, where drainage control is not done or not done inefficient way (OLIVEIRA, 1997). In the semi-arid Northeast there are currently large areas with salinized soils, due to the physical and chemical nature of the soils, water

deficit and high evaporation rate, with higher incidence of the problem in the most intensively cultivated land using irrigation, in the agricultural poles irrigated (SILVA et al., 2011).

The factors directly responsible for soil salinization in irrigated areas are the use of irrigation water with high saline concentration, increased water table due to inadequate irrigation management, absence or deficiency of drainage, increased water table due to loss of water, water by infiltration into canals and reservoirs and, or, accumulation of irrigation water in the lower parts of the land (GHEYI et al., 1997).

Another factor also responsible for the induction of salinity is the excessive application of high saline fertilizers, such as potassium chloride, ammonium nitrate and commercial formulations, in an indiscriminate and excessive manner, which may induce an increase in osmotic pressure in the solution soil, affecting seed germination and the development of very young plants (FIGUEIRÊDO, 2005; WANDERLEY, 2009).

In this sense, salinity is one of the major limiting factors for plant development and productivity, being considered the major abiotic stress (ALLAKHVERDIEV et al., 2000). There are two types of salinity: primary, considered a natural process in areas where there is little rainfall and high evaporation, as well as gradual accumulation of ions from weathering (arid regions); and the secondary, resulting from an anthropic process, mainly by brackish water irrigation (WILLIAMS, 1987).

The effect of salinity on plants is conditioned by two components: osmotic stress and ionic stress. The first results from the elevation of solutes in the soil solution, causing a water deficit by reducing the osmotic potential; and the second is due to the high tissue Na^+ contents and the alteration of the K^+/Na^+ ratio, as well as the nutritional imbalance (MUNNS; TESTER, 2008). Still within the context of the osmotic effect of salinity, it is observed that plants have rapid inhibition of young leaf expansion, reduced stomatal conductance and leaf senescence at high Na^+ concentrations (FRICKE, 2002).

Evolutionarily, plants that have adapted to environments with a high concentration of salts have been derived from halophyte plants. These plants can tolerate concentration levels above 300-1000 mM of salt (ZHU, 2007) through the ability to compartmentalize sodium and accumulate osmolytes, keeping potassium concentrations constant. Halophyte plants can accumulate more salt in the leaves and roots, and can force sodium through the tonoplast with highly selective protein transporters for Na^+/K^+ (RADYUKINA et al., 2007). Most halophytes respond to salinity by exclusion (YADAV et al., 2011), and yet, plants must absorb salt under saline stress and store it in vacuoles or tissues where their damage is minimal or segregated. Secretion occurs through the elimination of salty leaves and also by salt glands, specialized

cells in the leaves and stem that secrete salt, which is carried by rain or wind (ASLAM et al., 2011)

Different from halophytes, plants considered glycophytes make up the majority of all plant life, including crops important to the world economy and food. These species do not tolerate saline stress and, contents above 100-200 mM of salt, can already cause the inhibition of growth and death of individuals (ZHU, 2007). On the other hand, it cannot be said that glycophytes do not have protective measures against these environmental conditions, instead, this group of plants even create a high K^+/Na^+ ratio through the active transport of ions, changing ionic gradients and electrochemicals to be more favorable to cytosolic processes (YADAV et al., 2011). Salt accumulates in Organs reproductive organs and leaves, and the plant focuses on mere survival rather than growth or reproduction (ZAKHARIN; PANICHKIN, 2009).

Plants under saline stress develop various strategies to tolerate saline stress to some extent, including morphological, physiological, biochemical and anatomical aspects, through alternative processes that include selective accumulation and / or exclusion of ions, control of the intake of root ions and leaf transport, compartmentalization of ions in the vacuoles, leaves, osmolytes synthesis, alteration of photosynthetic pathways and induction of antioxidant enzymes (IVENGA and REDDY, 1996; MUNNS, 2002).

Na^+ removal from cytoplasm is performed by Na^+/H^+ antiport proteins that use H^+ pumps to regulate the expression and activity of K^+ and Na^+ transporters, and under optimal conditions the plants present high K^+ concentration, which acts on enzymatic activation, stomatal opening and closing, among other functions, and low Na^+ concentration. Already in salinity conditions, K^+ levels decrease in the plant (ZHU et al., 1993). In general, Na^+ toxicity is most noticeable in the leaf blade, where Na^+ accumulates due to the process of leaf transpiration, while in roots Na^+ accumulation is more prominent in the epidermis, as it has direct contact with the soil solution and in the central cylinder (MUNNS, 2002).

The general hypothesis of the work considers the deleterious effects promoted by saline stress on anatomical responses. In other hand, root, stem and leaf anatomical modifications may contribute to compartmentation, minimizing salt transport on tissues. The general aim of this research was to evaluate the structural behavior using root, stem and leaf variables, detailing the possible anatomical modifications involved in these organs, as well as to understand the behavior of photosynthetic machinery, gas exchange, antioxidant system and oxidative damage in soybean plants subjected to progressive salt stress. For this, the thesis was divided into two chapters and the data structured according to submission guidelines.

The hypothesis of the first article considered the deleterious effects of salt stress on plant metabolism. In other words, the anatomical modifications linked to the root and stem can minimize the negative impacts caused by Na^+. The aim of this research was to evaluate the structural behaviour of the roots and stems, detailing possible anatomical modifications in these organs in soybean plants under progressive salt stress. The results published in Plant Biology.

The hypothesis of the second article was based on problems caused by saline stress on structural responses. Additionally, the anatomical modifications linked to leaves can contribute to the reduction of excessive transpiration and consequently minimize salt transport within the plant. The aim of this research was to evaluate the physiological, biochemical and nutritional effects and how they affect the structural characteristics in soybean plants subjected to progressive salt stress. The results expected to be published in Journal of Plant Growth Regulation.

REFERENCES

AGRIANUAL. **Anuário Estatístico da Agricultura Brasileira**. São Paulo: FNP – Consultoria & Agroinformativos, 409-444, 2015.

ALLAKHVERDIEV, S. I.; SAKAMOTO, A.; NISHIYAMA, Y.; INABA, M.; MURATA, N. Ionic and osmotic effects of NaCl-induced inactivation of photosystems I and II in *Synechococcus sp*. **Plant Physiology**, v. 123, p. 1047–1056, 2000.

ASLAM, R.; BOSTAN, N.; NABGHA-E-AMEN, MARIA, M.; SAFDAR, W. A critical review on halophytes: Salt tolerant plants. **J Med Plants Res**, v. 5, p. 7108-7118, 2011.

BORÉM, A. **Melhoramento de espécies cultivadas**. 1. ed Viçosa: Ed. UFV, p. 817, 1999.

BORÉM, A. **Melhoramento de espécies cultivadas**. 2. ed. Viçosa: Ed. UFV, p. 969, 2005.

BRUNINI, M. A.; BARROS, M. A. L.; PEREIRA, M.; CERQUEIRA, J. B.; MENEZES, P. T. R.; FURTADO, I. R. Qualidade de grãos de onze cultivares de soja. **Nucleus Animalium**, v. 8, n. 2, p. 55-62, 2016.

CAPELLARI JUNIOR, L.; RODRIGUES, R. R.; SOUZA, V. C. **Botânica sistemática aplicada aos cursos de engenharia agronômica e engenharia florestal**. Piracicaba: ESALQ-LCB, p. 103, 2007.

CONAB. Companhia Nacional De Abastecimento . Acompanhamento da safra brasileira de grãos. 1(1):2019. Disponível em <http://www.conab.gov.br>. Acesso em 16 de dezembro 2019.

FAGAN, E. B.; DOURADO NETO, D.; VIVIAN, R.; FRANCO, R. B.; YEDA, M. P.; MASSIGNAM, L. F.; MARTINS, K. V. Efeito da aplicação de piraclostrobina na taxa fotossintética, respiração, atividade da enzima nitrato redutase e produtividade de grãos de soja. **Bragantia**, v. 69, n. 4, p. 771- 777, 2010.

FAO. **Faostat Database Gateway - 2019**. Disponível em: <http://www.fao.org>. Acesso em: 18, dezembro, 2019.

FARIAS, J. R. B.; NEPOMUCENO, A. L.; NEUMAIER, N. **Ecofisiologia da soja. (Circular Técnica 48)**. Londrina: Embrapa Soja, 2007. 9 p.

FIGUEIRÊDO, A. F. R. **Análise do risco de salinização dos solos da bacia hidrográfica do Rio Colônia – Sul da Bahia**. 2005. 84 f. (Dissertação de Mestrado) – Universidade Estadual de Santa Cruz, Ilhéus.

FREITAS, M. C. M. A cultura da soja no Brasil: o crescimento da produção brasileira e o surgimento de uma nova fronteira agrícola. **Enciclopédia biosfera**, v. 7, n. 12, 2011.

FRICKE, W.; PETERS, W. S. The biophysics of leaf growth in salt-stressed Barley. A study at the cell level. **Plant Physiology**, v. 129, p. 374–388, 2002.

GHEYI, H. R.; QUEIROZ, J. E.; MEDEIROS, J. F. **Manejo e controle da salinidade na agricultura irrigada**. Campina Grande: UFPB/SBEA. 1997. 383p.

GHEYI, H. R. Problemas de salinidade na agricultura irrigada. In: OLIVEIRA, T.; ASSIS, J. R.; R. N.; ROMERO, R. E.; SILVA, J. R. C. (Eds.). **Agricultura, sustentabilidade e o semiárido**. Viçosa: Sociedade Brasileira de Ciência do Solo. 2000, p 329-345.

IBGE - Instituto Brasileiro De Geografia E Estatística. Levantamento sistemático da produção agrícola. Rio de Janeiro, 2016. 83 p. Disponível em http://www.ibge.gov.br. Acesso em 20 de dezembro 2016.

IYENGAR, E. R. R.; REDDY, M. P. Photosynthesis in highly salt tolerant plants. In: M. Pesserkali (ed.). **Handbook of photosynthesis**. Marshal Dekar, Baten Rose, USA. 1996. 952 p.

LEE, G. A.; CRAWFORD, G. W.; LIU, L.; SASAKI, Y.; CHEN, X. Archaeological soybean (*Glycine max*) in East Asia: does size matter?. **PloS one**, v. 6, n. 11, p. e26720, 2011.

MATTOS, E. C.; ATUI, M. B.; SILVA, A. M.; FERREIRA, A. R.; NOGUEIRA, M. D.; SANTOS SOARES, J.; MARCIANO, M. A. M. Estudo da identidade histológica de subprodutos de soja (*Glycine max L.)*. **Revista do Instituto Adolfo Lutz**, v. 74, n. 2, p. 104-110, 2016.

MISSÃO, M. R. Soja: origem, classificação, utilização e uma visão abrangente do mercado. **Maringá Management: Revista de Ciências Empresariais**, v. 3, n. 1, p. 7-15, 2006.

MUNNS, R. Comparative physiology of salt and water stress. **Plant, Cell & Environment**, v. 25, p. 239–250, 2002.

MUNNS, R.; TESTER, M. Mechanisms of Salinity Tolerance. **Annual Review of Plant Biology**, v. 59, p. 651–681, 2008.

MUSSKOPF, C.; BIER, V. A. Efeito da aplicação de fertilizante mineral cálcio e boro via foliar na cultura da soja (*Glycine Max*). **Cultivando o Saber**, v. 3, n. 4, p. 83-91, 2010.

NICOLOSO, R. D. S.; CARNEIRO AMADO, T. J.; SCHNEIDER, S.; ENÍVAR LANZANOVA, M.; CAUDURO GIRARDELLO, V.; BRAGAGNOLO, J. Eficiência da escarificação mecânica e biológica na melhoria dos atributos físicos de um Latossolo muito argiloso e no incremento do rendimento de soja. **Revista Brasileira de Ciência do Sol**o, v. 32, n. 4, p. 1723-1734, 2008.

OLIVEIRA, M. Gênese, classificação e extensão de solos afetados por sais. In: GUEYI, H. R.; QUEIROZ, J. E.; MEDEIROS, J. F. (Ed.) **Manejo e controle da salinidade na agricultura irrigada**. Campina Grande: UFPB, 1997, p.1-35.

PEDROTTI, A.; CHAGAS, R. M.; RAMOS, V. C.; PRATA, A. P. N.; LUCAS, A. A. T.; SANTOS, P. B. Causas e consequências do processo de salinização dos solos. **Revista Eletrônica em Gestão, Educação e Tecnologia Ambiental**. v. 19, n. 2, p. 1308-1324, 2015.

RADYUKINA, N. L.; KARTASHOV, A. V.; IVANOV, Y. V.; SHEVYAKOVA, N. I.; KUZNETSOV, V. V. Functioning of defense systems in halophytes and glycophytes under progressing salinity. **Russ J Plant Physl**, v. 54, p. 806-815, 2007.

RENNÓ, F. P; CÔNSOLO, N. R. B; BARLETTA, R. V; VENTURELI, B.; GARDINAL, R.; TAKIYA, C. S; GANDRA, J. R; E PEREIRA, A. S. C. Grão de soja cru e inteiro na alimentação de bovinos: Excreção de grão de soja nas fezes. **Arch. Zootec.** v. 64, n. 248, p. 331-338, 2015.

RIBEIRO, M. R.; FREIRE, F. J.; MONTENEGRO, A. A. A. 2003. Solos halomórficos no Brasil: Ocorrência, gênese, classificação, uso e manejo sustentável. In: CURI, N.; MARQUES, J. J.; GUILHERME, L. R. G.; LIMA, J. M.; LOPES, A. S; ALVAREZ, V. H. (eds.). **Tópicos em Ciência do Solo**. Viçosa: Sociedade Brasileira de Ciência do Solo. 2003, v. 3, p. 165-208.

ROCHA, R. S. **Avaliação de variedades e linhagens de soja em condições de baixa latitude**. p. 61, 2009. Dissertação (Mestrado em Produção Vegetal), Universidade Federal do Piauí, 2009.

SEDIYAMA, T. **Tecnologias de produção e usos da soja**. 1. ed. Londrina, PR: Mecenas, v. 1, p. 314, 2009.

SILVA, J. L. A.; ALVES, S. S. V.; NASCIMENTO, I. B.; SILVA, M. V. T.; MEDEIROS, J. F. 2011. Evolução da salinidade em solos representativos do Agropólo Mossoró-Assu cultivado com meloeiro com água de deferentes salinidades. **Agropecuária Científica no Semiárido**. v. 7, n. 4, p. 26-31.

SOUSA. C. H. C. **Análise da tolerância a salinidade em plantas de sorgo, feijão de corda e algodão**. 2007. 73 f. Dissertação (Mestrado em Irrigação e Drenagem) - Universidade Federal do Ceará, Fortaleza.

SOUZA, V. Q.; NARDINO, M.; FOLLMANN, D. N.; BAHRY, C. A.; CARON, B. O.; ZIMMER, P. D. Caracteres morfofisiológicos e produtividade da soja em razão da desfolha no estádio vegetativo. **Científica**, v. 42, n. 3, p. 216-223, 2014.

STACHIW, R.; RIBEIRO, S. B.; JARDIM, M. A. G.; POSSIMOSER, D.; ALVES, W. C.; CAVALHEIRO, W. C. S. Potencial de produção de biodiesel com espécies oleaginosas nativas de Rondônia, Brasil. **Acta Amazonica**. v. 46, n. 1, p. 81-90, 2016.

WANDERLEY, R. A. **Salinização de solos sob aplicação de rejeito de dessalinizadores com e sem adição de fertilizantes**. 2009. 52 f. (Dissertação de Mestrado) – Universidade de Federal Rural de Pernambuco, Recife.

WILLIAMS, W. D. Salinization of rivers and streams: an important environmental hazard. **Ambio**. v. 16, p. 180-185, 1987.

YADAV, S.; IRFAN, M.; AHMAD, A.; HAYAT, S. Causes of salinity and plant manifestations to salt stress: A review. **J Environ Biol**, v. 32, p. 667-685, 2011.

ZAKHARIN, A. A.; PANICHKIN L. A. Glycophyte salt resistance. **Russ J Plant Physl**, v. 56, p. 94-103, 2009.

ZAKIR, M. M.; FREITAS, I. R. Benefícios à saúde humana do consumo de isoflavonas presentes em produtos derivados da soja. **J. Bioen. Food Sci.** v. 2, n. 3, p. 107-116, 2015.

Zhu, J. K. **Plant salt stress**. *In* Encylcopedia of Life Sciences. John Wiley & Sons, Ltd. 2007

ZHU, J. K.; SHI, J.; SINGH, U.; WYATT, S. E.; BRESSAN, R. A.; HASEGAWA, P. M.; CAPITA, N. C. Enrichment of vitronectin and fibronectin like proteins in NaCl-adapted plant cells and evidence for their involvement in plasma membranecell wall adhesion. **The Plant Journal**. v. 3, p. 637–646, 1993.

plant biology

Plant Biology ISSN 1435-8603

RESEARCH PAPER

Anatomical changes in stem and root of soybean plants submitted to salt stress

B. R. S. Silva[1], B. L. Batista[2] & A. K. S. Lobato[1]

1 Núcleo de Pesquisa Vegetal Básica e Aplicada, Universidade Federal Rural da Amazônia. Paragominas, Pará, Brazil

2 Centro de Ciências Naturais e Humanas, Universidade Federal do ABC, Santo André, São Paulo, Brazil

Keywords
Cambium; *Glycine max*; Na^+ exclusion; salinity; vascular cylinder.

Correspondence
A. K. S. Lobato, Rodovia PA 256, Paragominas, Pará, Brazil. Núcleo de Pesquisa Vegetal Básica e Aplicada, Universidade Federal Rural da Amazônia.
E-mail: allanllobato@yahoo.com.br

Editor
Z.-B. Luo

Received: 30 April 2020; Accepted: 3 August 2020

doi:10.1111/plb.13176

ABSTRACT

- The soybean is a legume that is widely cultivated in many countries due to the high levels of protein and oil contained in its seed, and is used for human and animal nutrition. However, salinity affects more than 800 million hectares worldwide, limiting global agricultural production.
- The aim of this research was to evaluate the structural behaviour of the roots and stems under progressive salt stress, detailing the possible anatomical modifications to these organs in soybean plants during this stress. The plants were randomized into five treatments (0, 50, 100, 150 and 200 mM NaCl).
- All the root regions studied and exposed to 100 mM Na^+ exhibited increases in the epidermis and endodermis and formation of lysogenic aerenchyma with increasing salinity, revealing the protective roles of these structures in reducing Na^+ influx. In the stem, increases in the cortex and pith in the first internode subject to 100 mM Na^+ suggest anatomical responses that aim to minimize oxidative stress.
- Soybean plants subjected to progressive salt stress (>50 mM Na^+) avoided cavitation and loss of function linked to vessel elements, reducing the metaxylem in all the root and stem regions analysed. Finally, our results confirm anatomical changes to the roots and stems.

INTRODUCTION

Soybean [*Glycine max* (L.) Merr.] is a legume that is widely cultivated in many countries due to the high levels of protein and oil contained in its seeds (Nishinari *et al.* 2014). Soybean is used for human and animal nutrition (Sanjukta & Rai 2016), industrial products and biofuel (Cavalett & Ortega 2010; Chen *et al.* 2012). According to the FAO (2017), the USA leads the world production of soybean, followed by Brazil and Argentina, with estimated production levels of 119, 114 and 54 million tons, respectively. However, high salt concentrations in the soil limit the worldwide agricultural production (Parihar *et al.* 2015), with more than 800 million hectares estimated to be affected by salinity worldwide (FAO 2017), representing a challenge to modern agriculture in glycophyte cultivation, such as soybean, in areas under saline conditions (Cheeseman 2015).

Salinity is one of the main forms of abiotic stress and occurs mainly in the arid and semiarid regions of the world (Abuelgasim & Ammad 2019). Limited rainfall in these regions, associated with low bioclimatic activity and low weathering, lead to the formation of soils with high salt concentrations (Hanin *et al.* 2016). Additionally, excess fertilizers, pesticides and inadequate irrigation management potentiate the salinization process (Manchanda & Garg 2008). Saline solution consists of a variety of dissolved salts, such as Na_2SO_4, $MgSO_4$, $CaSO_4$, $MgCl_2$, KCl, Na_2CO_3 and NaCl; NaCl is the most common salt and the target of most studies on salinity (Munns & Tester 2008).

Salt stress promotes several deleterious effects (Acosta-Motos *et al.* 2017), including reduction of leaf area, negative regulation of photosynthesis (Agrawal *et al.* 2013), stomatal closure and overproduction of reactive oxygen species (ROS) (Hussain *et al.* 2016), resulting in chlorosis and leaf senescence (Phang *et al.* 2008). In the short term, osmotic stress induced by Na^+ decreases water availability in the plant. In the long term, toxicity occurs through ionic imbalance (Horie *et al.* 2012), mainly by the replacement of K^+ by Na^+ in the cytosol, negatively interfering with homeostasis, including the K^+/Na^+ ratio. Potassium deficiency impacts development of the root components (Sustr *et al.* 2019), such as the metaxylem, which is essential to uptake of water and nutrients (Oliveira *et al.* 2019), also affecting biochemical reactions and protein conformations that depend of this element as a cofactor during protein biosynthesis (Zhu 2002).

Stress induced by Na^+ causes structural changes to plants, including changes in important plant organs, such as roots and stems (Barberon *et al.* 2016). In roots, this stress often reduces the elongation rate (Potters *et al.* 2007; Deinlein *et al.* 2014), creates disorders of root architecture (Julkowska *et al.* 2014), interferes with gravity responses, induces halotropism (Sun *et al.* 2008) and anatomical modifications, including decreased cell expansion, delayed cell division and impaired differentiation (Robin *et al.* 2016). In stems, there is a reduction in height to minimize salt uptake, maximization of cutin synthesis in epidermal cells, lignification of cells and disorders in xylem structure (Dolatabadian *et al.* 2011; Nja et al. 2018). Specifically in soybean plants, salt stress negatively affects the stem cortex (Dolatabadian *et al.* 2011), significant reducing the length of roots (Shu *et al.* 2017), leading to lower biomass in root and

stem tissues (Alam *et al.* 2019) and consequent increments in cell death (Egbichi *et al.* 2014).

Anatomical modifications represents an important strategy in plant survival in an environment affected by salinity; in this process, structures linked to roots and stems are modified depending on the exposure time and the intensity of salinity. In the root, mild or moderate salt stresses the epidermis and endodermis cells, where root vessel elements become thickened in order to prevent Na^+ accumulation in this organ (Choat *et al.* 2010). Under severe salinity conditions, the inverse behaviour occurs due to the deleterious effects caused by excess Na^+, affecting cell expansion and cell wall integrity (Sellami *et al.* 2019). In stems, mild or moderate saline stress promotes an increase in the amount of parenchyma cells, contributing to the compartmentalization of this ion into vacuoles (Horie *et al.* 2012), while severe salt stress creates a decrease in parenchyma cells that can be related to unfavourable osmotic conditions and inhibition of cell differentiation (Zhang *et al.* 2016).

Our hypothesis considered the deleterious effects of salt stress on plant metabolism. In other words, the anatomical modifications linked to the root and stem can minimize the negative impacts caused by Na^+. The aim of this research was to evaluate the structural behaviour of the roots and stems, detailing possible anatomical modifications in these organs in soybean plants under progressive salt stress.

MATERIAL AND METHODS

Location and growth conditions

The experiment was performed on the campus of Paragominas of the Universidade Federal Rural da Amazônia, Paragominas, Brazil (2°55′ S, 47°34′ W). The study was conducted in a greenhouse in which the temperature and humidity were controlled. The minimum, maximum and median temperatures were 27.7, 28.9 and 26.3 °C, respectively. The relative humidity during the experimental period varied between 60% and 80%.

Plants, containers and acclimation

Seeds of *Glycine max* (L.) Merr. var. M8644RR Monsoy™ were germinated and grown in 1.2-l pots filled with a mixed substrate of sand and vermiculite at a ratio of 3:1. The plants were cultivated under semi-hydroponic conditions containing 500 ml distilled water for 8 days. A modified Hoagland & Arnon (1950) solution was used for nutrients, with the ionic strength starting at 50% (day 6) and later being modified to 100% after 2 days (day 8). After this period, the nutrient solution remained at total ionic strength.

Experimental design

Plants were maintained entirely randomized into five treatments (0, 50, 100, 150 and 200 mM NaCl, described as 0, 50, 100, 150 and 200 mM Na^+, respectively). Five replicates of each treatment were conducted, producing a total of 25 experimental units (pots), with one plant in each unit. These Na^+ concentrations were defined based on the studies conducted by He *et al.* (2014) and Liu *et al.* (2016), both using soybean plants.

Plant conditions and salt stress

Plants received macro- and micronutrients using aerated nutrient solution as in Oliveira *et al.* (2019). To simulate Na^+ exposure, NaCl was used at concentrations of 0, 50, 100, 150 and 200 mM Na, applied over 15 days (days 20–35 after the start of the experiment). On day 35 of the experiment, physiological and morphological parameters were measured for all the plants, and leaf tissues were harvested for anatomical, biochemical and nutritional analyses.

Measurements of anatomical parameters

Samples were collected from the root apex and fragments from 5, 10 and 15 cm from the root apex and middle region of the 1st, 2nd and 3rd internode. Subsequently, all the collected materials were fixed in FAA 70 for 24 h, dehydrated in ethanol and embedded in Historesin (Leica, Nussloch, Germany). Transverse and longitudinal sections with a thickness of 5 μm were obtained using a rotating microtome (model Leica RM 2245; Leica). The sections were stained with toluidine blue (O'Brien *et al.* 1964). Some sections were analysed in polarized light to visualize the cellular constituents of birefringent nature.

Scanning electron microscopy (SEM)

The root apex previously fixed in FAA was dehydrated in an ethyl series, processed in a critical point CO_2 dryer and metallized with gold (layer approximately 20-nm thick) under a current of 25 mA. The micrographs were obtained using scanning electron microscopy (model LEO 1450 VP, Zeiss).

Determination of Na+ and K+

Quantifications of Na^+ and K^+ in root and stem tissues were carried out using an inductively coupled plasma mass spectrometer (model ICP-MS 7900; Agilent, USA) in agreement with procedures described by Paniz *et al.* (2018).

Measurements of morphological parameters

The biomass of roots and stems was measured based on constant dry weights (g) after drying in a forced-air ventilation oven at 65 °C.

Data analysis

The data were subjected to ANOVA, and significant differences between the means were determined using the Scott-Knott test at a probability level of 5% (Steel *et al.* 2006). Standard deviations were calculated for each treatment.

RESULTS

Sodium and K^+ content in root and stem

Salt stress caused significant modifications to the Na^+ content in the vegetative organs (Table 1), with values of 19 to 22 mg·g·DM^{-1} (root), ranging from 15.6 to 55.6 mg·g·DM^{-1} in the stem under 50, 100, 150 and 200 mM Na^+, compared to

Table 1. Na^+ and K^+ contentsand K^+/Na^+ ratio in soybean plants submitted to salt stress.

Na^+ (mM)	Na^+ in root (mg·g·DM^{-1})	Na^+ in stem (mg·g·DM^{-1})
0	2.47 ± 0.18c	0.16 ± 0.03e
50	19.04 ± 1.68b	15.64 ± 0.10d
100	20.85 ± 0.82a	46.23 ± 1.92c
150	21.71 ± 1.99a	54.16 ± 0.90b
200	22.26 ± 2.17a	55.62 ± 0.63a
Na^+ (mM)	K^+ in root (mg·g·DM^{-1})	K^+ in stem (mg·g·DM^{-1})
0	27.78 ± 2.17a	62.47 ± 1.29a
50	15.45 ± 0.99b	37.72 ± 0.91b
100	10.48 ± 0.33c	23.82 ± 1.08c
150	8.72 ± 0.45d	12.98 ± 0.16d
200	7.76 ± 0.17e	10.03 ± 0.05e
Na^+ (mM)	K^+/Na^+ in root	K^+/Na^+ in stem
0	11.25 ± 0.30a	382.61 ± 20.57a
50	0.81 ± 0.03b	2.41 ± 0.07b
100	0.50 ± 0.03c	0.51 ± 0.04c
150	0.40 ± 0.04d	0.24 ± 0.02d
200	0.35 ± 0.02d	0.18 ± 0.01e

Columns with different letters indicate significant differences from the Scott-Knott test ($P < 0.05$). Values described are means from five repetitions ± SD.

the control. In relation to K^+ content (Table 1), plants exposed to 50, 100, 150 and 200 mM Na^+ suffered decreases ($P < 0.05$) of 44%, 62%, 69% and 72% (root) and 40%, 62%, 79% and 84% (stem), respectively, compared with the control treatment (0 mM Na^+). The K^+/Na^+ ratios confirmed intense reductions (Table 1), which oscillated in roots (93%–97%) and stems (99.4%–99.7%) under 50 to 200 mM Na^+ in comparison to the control.

Anatomical changes linked to root after salt stress

Sodium stress promoted significant differences in root epidermis and endodermis thickness, cortex thickness, vascular cylinder diameter and metaxylem diameter at different root depths, with increases at 50 and 100 mM Na^+ and decreases at 150 and 200 mM Na^+ treatment (Table 2). For the root epidermis thickness and metaxylem diameter (5 cm from apex), there were increases of 53% and 112%, respectively, under 50 mM Na^+, but reductions of 44% and 57% under 200 mM Na^+, compared to the control treatment (0 mM Na^+). For root endodermis thickness (10 cm from apex), treatment with 100, 150 and 200 mM Na^+ resulted in decreases of 2%, 7% and 56%, respectively, while treatment with 50 mM Na^+ caused an increase of 17% compared to the control. For root cortex thickness and vascular cylinder diameter (15 cm from apex), there were increases of 28% and 64%, respectively, under 100 mM Na^+, but decreases of 8% to 17%, respectively, under 200 mM Na^+ compared to the control (Figs 1 and 2). The root exhibited structural changes in all regions analysed, and these changes increased with the addition of Na^+ in relation to control plants. The root apex was reduced in the size and thickness of the root cap (Fig. 3). In cross-sections, the regions at 5, 10 and 15 cm from the root apex showed lysogenic aerenchyma, thickening of the cell walls and cells with plasmolysed parenchyma. In the vascular cylinder, there was a reduction in cell size and deformation of vessel elements (Fig. 2).

Modifications induced by progressive salt stress in stems

Salt stress caused significant changes in the internodal regions studied (Table 3). Plants subjected to concentrations of 50–200 mM Na^+ had significant reductions in the second internode, which fluctuated in stem epidermis thickness (28%–51%) and cambium thickness (37%–82%) compared to the control (0 mM Na^+). For stem cortex thickness, phloem thickness, xylem thickness and metaxylem diameter (50 mM Na^+), there were increases of 65%, 50%, 36% and 42% in the first internode, respectively; however, treatment with 200 mM Na^+ resulted in decreases of 62%, 56%, 58% and 47%, respectively, compared to the control. For the first internode of stem pith diameter, there were increases of 20% in plants treated with

Table 2. Root anatomy in soybean plants subjected to salt stress.

Na^+ (mM)	RET (μm)	RDT (μm)	RCT (μm)	VCD (μm)	RMD (μm)
5 cm from apex					
0	16.9 ± 1.1b	23.9 ± 2.0b	385.5 ± 37.1a	332.7 ± 32.2a	63.2 ± 4.7b
50	25.9 ± 2.3a	33.1 ± 3.1a	289.9 ± 8.2b	265.0 ± 12.5b	133.7 ± 8.9a
100	13.1 ± 1.2c	21.7 ± 1.8b	269.7 ± 9.6b	237.6 ± 14.4c	32.5 ± 2.7c
150	11.9 ± 1.0c	19.6 ± 1.4c	228.7 ± 13.3c	213.5 ± 18.5d	31.7 ± 2.2c
200	9.4 ± 0.7d	16.4 ± 1.5d	199.4 ± 14.4d	206.1 ± 5.7d	27.1 ± 2.1c
10 cm from apex					
0	11.2 ± 0.8b	20.7 ± 1.8b	289.0 ± 12.5a	251.7 ± 4.9b	42.6 ± 3.9c
50	12.2 ± 0.7b	24.3 ± 1.6a	293.9 ± 13.6a	257.2 ± 9.4b	53.1 ± 2.2b
100	13.7 ± 1.3a	20.3 ± 1.6b	207.8 ± 10.7b	401.4 ± 9.7a	64.1 ± 4.9a
150	11.0 ± 0.9b	19.3 ± 1.4b	195.9 ± 18.3b	263.7 ± 17.1b	39.9 ± 3.2c
200	10.9 ± 1.1b	9.2 ± 0.8c	190.4 ± 18.6b	238.7 ± 18.8b	38.7 ± 1.7c
15 cm from apex					
0	11.9 ± 1.1a	20.5 ± 1.9b	205.6 ± 8.8b	310.5 ± 30.4b	55.3 ± 4.8b
50	12.3 ± 1.0a	25.4 ± 2.8a	216.4 ± 15.3b	335.2 ± 11.4b	67.0 ± 4.7a
100	13.3 ± 0.9a	19.0 ± 1.2b	263.6 ± 26.1a	510.7 ± 44.4a	44.4 ± 4.3c
150	10.7 ± 0.9b	17.9 ± 1.5b	200.9 ± 15.5b	273.6 ± 21.5c	37.4 ± 3.3d
200	9.8 ± 0.7b	13.9 ± 1.0c	190.0 ± 18.6b	258.2 ± 16.4c	33.3 ± 2.3d

Columns with different letters indicate significant differences from the Scott-Knott test ($P < 0.05$). Values are means of five repetitions ± SD. RET = Root epidermis thickness; RDT = Root endodermis thickness; RCD = Root cortex thickness; VCD = Vascular cylinder diameter; RMD = Root metaxylem diameter.

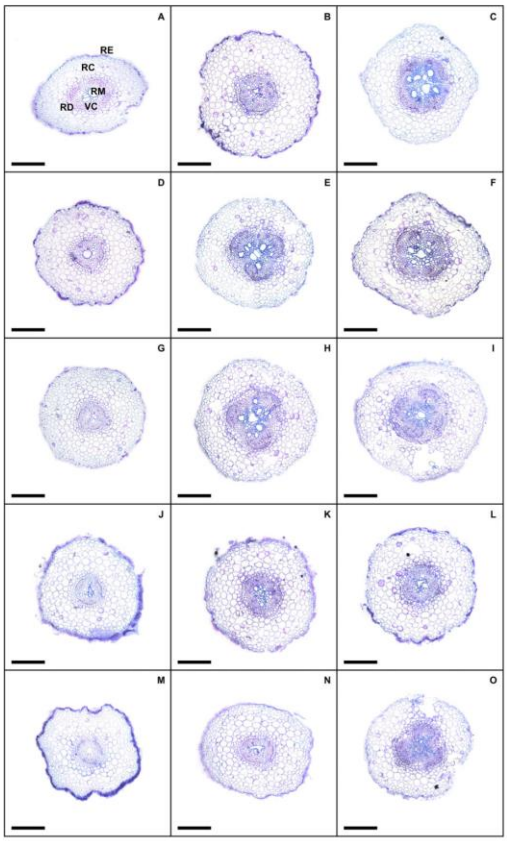

Fig. 1. Transverse section of roots from 5 cm (A, D, G, J and M), 10 cm (B, E, H, K and N) and 15 cm (C, F, I, L and O) from the apex in soybean plants subjected to salt stress. 0 mM Na+ (A, C), 50 mM Na+ (D, F), 100 mM Na+ (G, I), 150 mM Na+ (J, L) and 200 mM Na+ (M, O). RE = root epidermis; RC = root cortex; RD = root endodermis; VC = vascular cylinder; RM = root metaxylem. Bars: 200 μm.

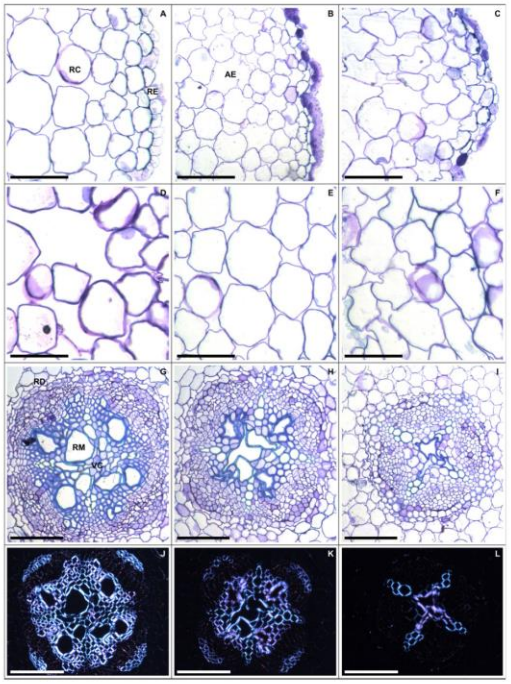

Fig. 2. Transverse section of roots showing aerenchyma formation in 5 cm from the apex (A, C), cortical region with plasmolyzed parenchyma cells in 10 cm from the apex (D, F) and vascular cylinder (G, I) and with polarized light (J, L) 15 cm from the apex in soybean plants subjected to salt stress. 0 mM Na+ (A, D, G and J), 100 mM Na+ (B, E, H and K), 100 mM Na+ (C and F) and 200 mM Na+ (I and L). RE = root epidermis; RC = root cortex; AE = aerenchyma; RD = root endodermis; VC = vascular cylinder; RM = root metaxylem. Bars: 50 μm (A C) and 200 μm (D, L).

100 mM Na^+ and a decrease of 18% in plants treated with 200 mM Na^+ compared to the control (Fig. 4). In the cross-section of the stem, the first internode had structural similarities at all analysed Na^+ concentrations (Fig. 5). However, under the 150 and 100 mM Na^+ treatments, the second and third internodes exhibited a delay in tissue development and cellular alterations, such as parenchyma cells with thin cell walls, plasmolysis, low activity in vascular cambium due to the presence of a discontinuous vascular cylinder, and immature phloem and secondary xylem cells.

Sodium negatively affects biomass

The plant biomass was significantly impacted by salt stress (Table 4). Plants exposed to Na^+ suffered reductions of 43%, 48%, 59% and 75% in roots and 51%, 65%, 78% and 78% in stems when exposed to 50, 100, 150 and 200 mM Na^+, respectively, compared to the control.

DISCUSSION

The increases in root and stem Na^+ content confirm the efficacy of the salt stress simulated in this study. In addition, concentrations above 100 mM NaCl revealed that Na^+ absorbed by the roots was transported and accumulated in the stem tissues. Under increased salt conditions, Na^+ uptake negatively affected the absorption of essential elements, including K^+, as confirmed in this research. Reductions in the K^+/Na^+ ratio after salt stress are intrinsically related to lower K^+ content in the tissues evaluated, resulting in an ionic imbalance that has a negative impact on metabolic activity (Hanin *et al.* 2016). There is a negative relationship between Na^+ and K^+, in which K^+ eflux represents a faster and more cost-effective method to estimate tolerance to salinity, as found in *Hordeum vulgare* (Chen *et al.* 2005). However, at high concentrations, the Na^+ influx into cells is frequently toxic to plant metabolism and, to minimize the effects on growth and development that can lead to cell death, excess Na^+ can be extruded or compartmentalized in the vacuole (Farooq *et al.* 2015). Oliveira *et al.* (2019) evaluated the homeostasis, antioxidant metabolism and leaf anatomy of *Eucalyptus urophylla* subjected to 250 mM NaCl and found

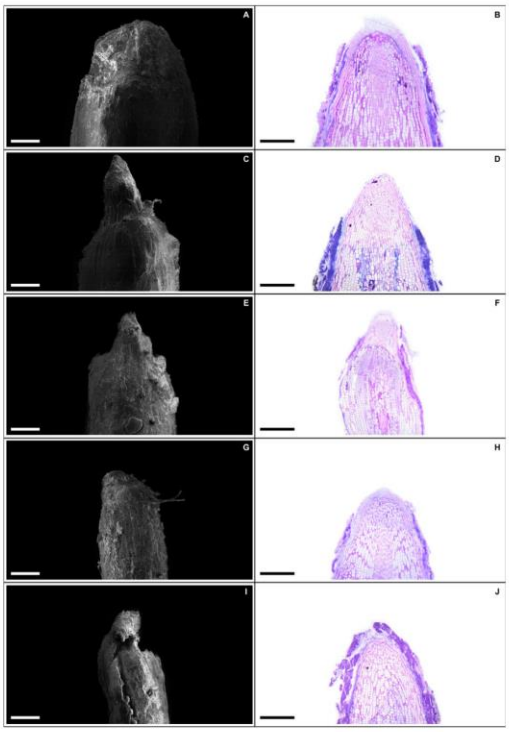

Fig. 3. Root apex analysed by scanning electron microscopy (A, C, E, G and I) and longitudinal section (B, D, F, H and J) in soybean plants subjected to salt stress. 0 mM Na+ (A, B), 50 mM Na+ (C, D), 100 mM Na+ (E, F), 150 mM Na+ (G H) and 200 mM Na+ (I, J). Bars: 200 μm.

increases in the Na^+ content in roots and stems. Rodrigues *et al.* (2014), studying the physiological adjustment of *Ricinus communis* exposed to 50, 100 and 150 mM NaCl, described NaCl increases of 6-, 11- and 19-fold in the roots and 18-, 19- and 20-fold in the stems, respectively, when compared to control plants (0 mM NaCl). Falakboland *et al.* (2017), working with 12 varieties of *Hordeun vulgare*, determined that the K^+ cation modulates tolerance to salt stress, and these authors suggested that this element is crucial for enzyme activation and protein synthesis stabilization. Wang *et al.* (2019), using two leaf types (cotyledon and true leaf) in *Ricinus communis* seedlings submitted to Na stress, proved that the K^+/Na^+ ratio is significantly affected, causing disorders in physiological processes.

The increases in root epidermis thickness, endodermis thickness and cortex thickness under mild and moderate salinity (50 and 100 mM Na^+) suggest resistance of the root tissues to simulated abiotic stress. In this context, the epidermis, endodermis and cortex represent a mechanical barrier in the radial transport of water and ions, such as Na^+, and prevent the reflux of solutes to protect the vascular tissues (Líška *et al.* 2016; Doblas *et al.* 2017). The vascular cylinder and metaxylem contribute to the conduction of water to the upper organs, and affect Na^+ efflux *via* conductive cells. Additionally, the partial increases observed in the vacuolar cylinder diameter and root metaxylem diameter (50 and 100 mM Na^+) suggest a plant strategy to improve water use efficiency and Na^+ exclusion in the shoot through Na^+ partition assimilation (Deinlein *et al.* 2014; Prince *et al.* 2017). On the other hand, under severe salinity (150 and 200 mM Na^+), there were reductions in all variables evaluated, and these results were clearly related to the deleterious effects of excess Na^+ on the roots, because the increase in concentration of this ion in the solution causes plasmolysis and reductions in the protective tissues (epidermis and endodermis). These responses contribute to the prevention of cavitation in

Table 3. Stem anatomy in soybean plants subjected to salt stress.

Na^+ (mM)	SET (μm)	SCT (μm)	SPhT (μm)	SXT (μm)	SMD (μm)	SCaT (μm)	SPD (μm)
1st internode							
0	20.4 ± 1.3a	102.0 ± 2.7b	38.4 ± 2.8b	133.9 ± 8.4b	30.7 ± 2.1b	[a]	842 ± 41c
50	16.9 ± 1.2b	168.1 ± 11.7a	57.5 ± 2.4a	182.0 ± 4.7a	43.7 ± 1.4a	[a]	917 ± 9b
100	12.1 ± 1.0c	97.5 ± 7.3b	56.4 ± 4.4a	129.2 ± 7.9b	23.0 ± 2.7c	[a]	1008 ± 43a
150	10.4 ± 0.8d	93.1 ± 8.1b	28.3 ± 1.9c	86.6 ± 3.4c	18.0 ± 1.2d	[a]	842 ± 75c
200	10.1 ± 0.4d	38.4 ± 3.5c	16.9 ± 1.9d	56.8 ± 3.9d	16.3 ± 0.9d	[a]	691 ± 62d
2nd internode							
0	19.2 ± 1.1a	195.9 ± 10.2a	94.0 ± 6.2a	341.2 ± 26.9a	97.9 ± 9.9a	57.9 ± 4.8a	3053 ± 213a
50	13.9 ± 1.1b	114.5 ± 8.9b	64.1 ± 4.4b	317.6 ± 14.1a	63.9 ± 2.6b	36.7 ± 3.2b	2259 ± 40b
100	11.9 ± 1.0c	88.3 ± 8.6c	46.9 ± 4.4c	257.9 ± 20.5b	47.0 ± 4.2c	26.9 ± 2.5c	1977 ± 45c
150	10.7 ± 0.7d	88.0 ± 5.8c	45.6 ± 3.0c	232.5 ± 16.9c	37.9 ± 2.6d	15.9 ± 0.7d	1502 ± 98d
200	9.4 ± 0.9d	87.0 ± 7.2c	35.5 ± 3.2d	142.3 ± 12.4d	32.2 ± 2.2d	10.6 ± 0.6e	1151 ± 71e
3rd internode							
0	16.2 ± 1.2a	161.6 ± 13.1a	103.0 ± 4.5a	405.8 ± 28.6a	123.7 ± 11.1a	58.8 ± 3.9a	3003 ± 103a
50	10.8 ± 0.8b	102.4 ± 6.6b	74.6 ± 2.1b	313.0 ± 30.4b	80.7 ± 1.9b	38.5 ± 3.6b	2595 ± 88b
100	10.2 ± 0.3b	88.4 ± 6.2c	70.8 ± 5.3b	288.8 ± 18.5b	56.1 ± 1.5c	29.6 ± 2.2c	2133 ± 60c
150	9.6 ± 0.7c	87.6 ± 2.3c	63.5 ± 2.7c	271.7 ± 1.9c	51.9 ± 1.0c	25.9 ± 1.0d	2094 ± 23c
200	8.9 ± 0.5c	86.3 ± 7.3c	57.1 ± 3.2d	250.5 ± 16.9d	50.5 ± 3.5c	22.5 ± 1.8d	2089 ± 113c

Columns with different letters indicate significant differences from the Scott-Knott test ($P < 0.05$). Values are means from five repetitions ± SD. SET = Stem epidermis thickness; SCT = Stem cortex thickness; SPhT = Stem phloem thickness; SXT = Stem xylem thickness; SMD = Stem metaxylem diameter; SCaT = Stem cambium thickness; SPD = Stem pith diameter.

[a]Cambium not included.

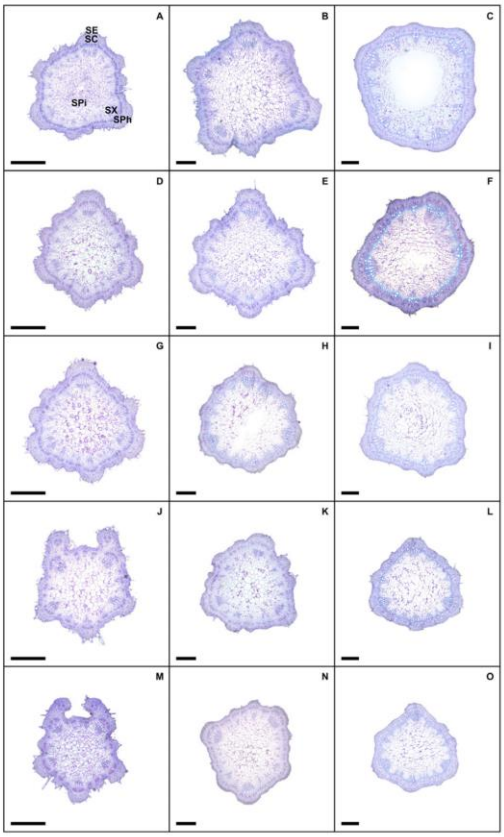

Fig. 4. Transverse section of the stem at the 1st internode (A, D, G, J and M), 2nd internode (B, E, H, K and N) and 3rd internode (C, F, I, L and O) in soybean plants subjected to salt stress. 0 mM Na+ (A, C), 50 mM Na+ (D, F), 100 mM Na+ (G, I), 150 mM Na+ (J, L) and 200 mM Na+ (M, O). SE = stem epidermis, SC = stem cortex, SPh = stem phloem, SX = stem xylem, SPi = stem pith. Bars: 500 µm (A, D, G, J and M) and 800 µm (B, C, E, F, H, I, K, L, N and O).

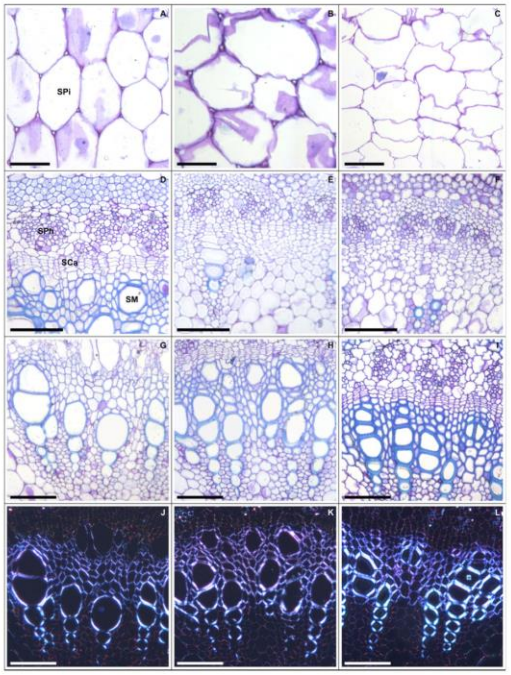

Fig. 5. Transverse section of the stem at the 2nd internode showing the pith region (A–C), vascular region (D, F) and the 3rd internode showing the vascular region (G, I) and with polarized light (J, L) in soybean plants subjected to salt stress. 0 mM Na+ (A, D, G, and J), 100 mM Na+ (B, E, H, and K) and 200 mM Na+ (C, F, I, and L). SPi = stem pith, SPh = stem phloem, SCa = stem cambium, SM = stem metaxylem. Bars: 50 µm (A, C) and 200 µm (D, L).

Table 4. Biomass in soybean plants subjected to salt stress.

Na^+ (mM)	root (g)	stem (g)
0	4.24 ± 0.09a	7.02 ± 0.36a
50	2.43 ± 0.04b	3.42 ± 0.18b
100	2.19 ± 0.05c	2.45 ± 0.18c
150	1.74 ± 0.02d	1.51 ± 0.11d
200	1.06 ± 0.03e	1.52 ± 0.09d

Columns with different letters indicate significant differences from the Scott-Knott test ($P < 0.05$). Values described are means from five repetitions ± SD.

the vascular cylinder and the subsequent loss of conductive cell functionality (Choat *et al.* 2010). Reductions in vascular cylinder diameter and root cortex thickness induced by salinity (150 and 200 mM) were observed by Hameed *et al.* (2009) who analysed anatomical adaptations of the thicker regions of adventitious roots of two *Imperata cylindrica* ecotypes.

The emergence of lysigenous aerenchyma under saline stress indicates a possible function of dead cells in preventing the influx of Na^+ ions, when this salt is in excess in the internal parts of the roots, with subsequent exclusion or ion impedence (Liu *et al.* 2007). Wang *et al.* (2010), studying *Thellungiella halophil*a subjected to 300 mM NaCl, found programmed and progressive cell death. In addition, cell wall thickening in cortical parenchyma cells is related to the frequent deposition of lignin and suberin to render them impermeable to water and ion passage (Purushothaman *et al.* 2013). Saqib *et al.* (2005) comparing two *Triticum aestivum* genotypes cultivated under saline conditions, described that the increased formation of root aerenchyma in the tolerant genotype induced a reduction in Na^+ content and increment of the K^+ concentration, improving the Na^+/K^+ ratio, Na^+ exclusion and salt tolerance. Akhtar *et al.* (2017) evaluating six *Typha domingensis* ecotypes often found in saline and/or polluted environments and exposed to progressive salt stress, confirmed significant increases in aerenchyma area of all ecotypes, in which this anatomical adaptation confers tolerance to salinity. Shen *et al.* (2014), studying different root regions in *Zea mays* seedlings subjected to 200 mM NaCl, described the thickening of cortex cells.

Regarding vessel elements, the irregularities observed under high concentrations (150 and 200 mM Na^+) of Na^+ reveal disturbances to the production of components, especially of the secondary cell wall, resulting in changes in the mechanical properties, making them susceptible to negative pressures and, consequently, interfering with water transport to other organs (Lefebvre *et al.* 2011; Bensussan *et al.* 2015). Sellami *et al.* (2019), studying the vascular anatomy of *Arabidopsis* exposed to salt stress (150 mM NaCl), detected xylem vessel deformations. For root cortex thickness and vascular cylinder diameter, the progressive reductions in the root apex and damage observed 5 cm from the apex corroborated that newly developed roots usually do not continue the normal processes of cell growth and elongation due to a lack of nutritional resources or an imbalance of ROS in this region (Jiang *et al.* 2016; Robin *et al.* 2016).

Under stress conditions, the stem epidermis contributes to the reduction in water loss *via* transpiration, and the reduction in stem epidermis thickness (>50 mM Na^+) represents the potential to increase plant tolerance to dehydration (Javelle *et al.* 2011). The partial increases in stem cortex thickness and pith diamter demonstrate that plants attempt to respond or tolerate mild and moderate salinity (50 and 100 mM Na^+) in meristematic regions. Thus, the cells that make up the cortex and pith can play a role in the storage of toxic ions, in this case Na^+, within their vacuoles or cytoplasm, as a way to attenuate the impact of this ion on the stem and to prevent cell damage (Horie *et al.* 2012). On the other hand, the reduction in stem cortex thickness and pith diameter found under high salt stress (150 and 200 mM Na^+) suggests a decrease in Na^+ uptake, causing unfavourable osmotic conditions and the appearance of plasmolized cells. Zhang *et al.* (2016), combining saline and alkaline stresses, found reductions in the stem epidermis thickness, cortex thickness and pith diameter in *Melilotus officinalis* subjected to 200 mM $NaHCO_3$.

The reductions observed in the stem cambium thickness, phloem thickness, xylem thickness and metaxylem diameter under severe salt conditions indicate that cambial activity was minimal, leading to a reduction of these tissues and favouring development of numerous narrow vessels in an attempt to reduce Na^+ transport (Zahra *et al.* 2014) but without compensating for larger vessel function (Boughalleb *et al.* 2009). The stem cambium is a secondary meristem responsible for radial growth, in which activity results in the differentiation of xylem and secondary phloem that mainly act in plant support, water conduction and photoassimilate transport between the roots and shoots (Risopatron *et al.* 2010). Nja et al. (2018), comparing the apical and basal internodes of *Medicago sativa* treated with 150 mM NaCl, observed reductions in stem phloem (6% and 3%) and xylem (20% and 14%) thickness.

Salinity affected plant growth, inducing reductions in the roots and stems. The lower biomass of plants exposed to Na^+ can have multiple causes, including reductions in root anatomical variables and delay in stem cambium differentiation. Under salt stress conditions, plants frequently exhibit reductions in biomass because the osmotic stress induced by Na^+ negatively interferes in the processes of cell division and elongation (Fricke & Peters 2002; Munns & Tester 2008), inhibiting root system development due to structural and functional restrictions; this limited development consequently impacts nutrient uptake and translocation (Zahra *et al.* 2014) and negatively affects light and CO_2 capture and stomatal regulation (Degl'Innocenti *et al.* 2009; Hussain *et al.* 2016). Qin *et al.* (2016), studying the interference of 100 mM NaCl on growth, the photosynthetic apparatus and cell ultrastructure, observed decreases in the roots and stems of *Vitis vinifera*. Yu *et al.* (2015) evaluated the effect of salinity on the morphological and nutritional characteristics, yield and composition of essential oils in *Mentha canadensis* and found progressive reductions in the roots and stems under NaCl concentrations of 0–150 mM.

CONCLUSIONS

This research showed that soybean plants subjected to progressive salt stress exhibited anatomical modifications to minimize the deleterious effects associated with Na^+. For all the root regions studied, increases in the epidermis and endodermis revealed the protective roles of these structures in plants subjected to 100 mM Na^+, reducing the Na^+ influx and the formation of lysogenic aerenchyma and increasing the salinity. In addition, dead cells are replaced by air spaces, thus minimizing the uptake of this toxic ion. Regarding the stems, there were increases in the cortex and pith in the first internode under concentrations of 100 mM Na^+, these being anatomical responses aiming to alleviate damage and oxidative stress generated by the salt in meristematic regions. Finally, all the root and stem regions analysed in the soybean plants subjected to concentrations of 50–200 mM Na^+ avoid cavitation and loss of function associated with vessel elements reducing the metaxylem, and this modification maximizes the impermeability of this tissue and prevents ionic flux due to increased cell wall thickness.

ACKNOWLEDGEMENTS

This research had financial support from Fundação Amazônia de Amparo a Estudos e Pesquisas (FAPESPA/Brazil), Conselho Nacional de Desenvolvimento Científico e Tecnológico (CNPq/Brazil) and Universidade Federal Rural da Amazônia (UFRA/Brazil) to AKSL. BRSS was supported by a scholarship from Coordenação de Aperfeiçoamento de Pessoal de Nível Superior (CAPES/Brazil). Additionally, we thank the Museu Paraense Emílio Goeldi (MPEG/Brazil) for the use of infrastructure for anatomical analysis.

AUTHOR CONTRIBUTIONS

AKSL was the advisor of this project and planned all phases of this research. BRSS conducted the experiment in the greenhouse and performed the physiological, anatomical, biochemical and morphological determinations, while BLB performed the nutritional determinations and helped draft the manuscript and interpret the results.

CONFLICT OF INTEREST

The authors declare that they have no competing interests.

Data Availability Statement

Data are available upon request to the corresponding author.

REFERENCES

Abuelgasim A., Ammad R. (2019) Mapping soil salinity in arid and semi-arid regions using Landsat 8 OLI satellite data. *Remote Sensing Applications: Society and Environment*, **13**, 415–425.

Acosta-Motos J.R., Ortuño M.F., Bernal-Vicente A., Diaz-Vivancos P., Sanchez-Blanco M.J., Hernandez J.A. (2017) Plant responses to salt stress: adaptive mechanisms. *Agronomy*, **7**, 1–38.

Agrawal R., Gupta S., Gupta N.K., Khandelwal S.K., Bhargava R. (2013) Effect of sodium chloride on gas exchange, antioxidative defense mechanism and ion accumulation in different cultivars of Indian jujube (*Ziziphus mauritiana* L.). *Photosynthetica*, **51**, 95–101.

Akhtar N., Hameed M., Nawaz F., Ahmad K.S., Hamid A., Segovia-Salcedo C., Shahnaz M.M. (2017) Leaf anatomical and biochemical adaptations in *Typha domingensis* Pers. ecotypes for salinity tolerance. *Botanical Sciences*, **95**, 807–821.

Alam P., Albalawi T.H., Altalayan F.H., Bakht M.A., Ahanger M.A., Raja V., Ashraf M., Ahmad P. (2019) 24-epibrassinolide (EBR) confers tolerance against NaCl stress in soybean plants by up-regulating antioxidant system, ascorbate-glutathione cycle, and glyoxalase system. *Biomolecules*, **9**, 640.

Barberon M., Vermeer J.E.M., De Bellis D., Wang P., Naseer S., Andersen T.G., Humbel B.M., Nawrath C., Takano J., Salt D.E., Geldner N. (2016) Adaptation of root function by nutrient-induced plasticity of endodermal differentiation. *Cell*, **164**, 447–459.

Bensussan M., Lefebvre V., Ducamp A., Trouverie J., Gineau E., Fortabat M.N., Guillebaux A., Baldy A., Naquin D., Herbette S., Lapierre C., Mouille G., Horlow C., Durand-Tardif M. (2015) Suppression of dwarf and Irregular Xylem phenotypes generates low-acetylated biomass lines in Arabidopsis. *Plant Physiology*, **168**, 452–463.

Boughalleb F., Denden M., Tiba B.B. (2009) Anatomical changes induced by increasing NaCl salinity in three fodder shrubs, *Nitraria retusa*, *Atriplex halimus* and *Medicago arborea*. *Acta Physiologiae Plantarum*, **31**, 947–960.

Cavalett O., Ortega E. (2010) Integrated environmental assessment of biodiesel production from soybean in Brazil. *Journal of Cleaner Production*, **18**, 55–70.

Cheeseman J.M. (2015) The evolution of halophytes, glycophytes and crops, and its implications for food security under saline conditions. *New Phytologist*, **206**, 557–570.

Chen K.I., Erh M.H., Su N.W., Liu W.H., Chou C.C., Cheng K.C. (2012) Soyfoods and soybean products: from traditional use to modern applications. *Applied Microbiology and Biotechnology*, **96**, 9–22.

Chen Z., Newman I., Zhou M., Mendham N., Zhang G., Shabala S. (2005) Screening plants for salt tolerance by measuring K^+ flux: a case study for barley. *Plant, Cell and Environment*, **28**, 1230–1246.

Choat B., Drayton W.M., Brodersen C., Matthews M.A., Shackel K.A., Wada H., Mcelrone A.J. (2010) Measurement of vulnerability to water stress-induced cavitation in grapevine: a comparison of four techniques applied to a long-vesseled species. *Plant, Cell & Environment*, **33**, 1502–1512.

Degl'Innocenti E., Hafsi C., Guidi L., Navari-Izzo F. (2009) The effect of salinity on photosynthetic activity in potassium-deficient barley species. *Journal of Plant Physiology*, **166**, 1968–1981.

Deinlein U., Stephan A.B., Horie T., Luo W., Xu G., Schroeder J.I. (2014) Plant salt-tolerance mechanisms. *Trends in Plant Science*, **19**, 371–379.

Doblas V.G., Geldner N., Barberon M. (2017) The endodermis, a tightly controlled barrier for nutrients. *Current Opinion in Plant Biology*, **39**, 136–143.

Dolatabadian A., Modarres Sanavy S.A.M., Ghanati F. (2011) Effect of salinity on growth, xylem structure and anatomical characteristics of soybean. *Notulae Scientia Biologicae*, **3**, 41–45.

Egbichi I., Keyster M., Ludidi N. (2014) Effect of exogenous application of nitric oxide on salt stress responses of soybean. *South African Journal of Botany*, **90**, 131–136.

Falakboland Z., Zhou M., Zeng F., Kiani-Pouya A., Shabala L., Shabala S. (2017) Plant ionic relation and whole-plant physiological responses to waterlogging, salinity and their combination in barley. *Functional Plant Biology*, **44**, 941–953.

FAO (2017) Food and Agriculture Organization of the United Nations FAOSTAT, Rome, Italy.

Farooq M., Hussain M., Wakeel A., Siddique K.H.M. (2015) Salt stress in maize: effects, resistance mechanisms, and management. A review. *Agronomy for Sustainable Development*, **35**, 461–481.

Fricke W., Peters W.S. (2002) The biophysics of leaf growth in salt-stressed barley. A study at the cell level. *Plant Physiology*, **129**, 374–388.

Hameed M., Ashraf M., Naz N. (2009) Anatomical adaptations to salinity in cogon grass [*Imperata cylindrica* (L.) Raeuschel] from the Salt Range, Pakistan. *Plant and Soil*, **322**, 229–238.

Hanin M., Ebel C., Ngom M., Laplaze L., Masmoudi K. (2016) New insights on plant salt tolerance mechanisms and their potential use for breeding. *Frontiers in Plant Science*, **7**, 1–17.

He Y., Yu C., Zhou L., Chen Y., Liu A., Jin J., Hong J., Qi Y., Jiang D. (2014) Rubisco decrease is involved in chloroplast protrusion and Rubisco-containing body formation in soybean (*Glycine max*) under salt stress. *Plant Physiology and Biochemistry*, **74**, 118–124.

Hoagland D.R., Arnon D.I. (1950) *The water-culture method for growing plants without soil*, 2nd edn. California Agricultural Experiment Station, Davis, CA, USA.

Horie T., Karahara I., Katsuhara M. (2012) Salinity tolerance mechanisms in glycophytes: an overview with the central focus on rice plants. *Rice*, **5**, 1–18.

Hussain M.I., Lyra D.A., Farooq M., Nikoloudakis N., Khalid N. (2016) Salt and drought stresses in safflower: a review. *Agronomy for Sustainable Development*, **36**, 1–31.

Javelle M., Vernoud V., Rogowsky P.M., Ingram G.C. (2011) Epidermis: the formation and functions of a fundamental plant tissue. *New Phytologist*, **189**, 17–39.

Jiang K., Moe-Lange J., Hennet L., Feldman L.J. (2016) Salt stress affects the redox status of Arabidopsis root meristems. *Frontiers in Plant Science*, **7**, 1–10.

Julkowska M.M., Hoefsloot H.C.J., Mol S., Feron R., De Boer G.J., Haring M.A., Testerink C. (2014) Capturing Arabidopsis root architecture dynamics with root-fit reveals diversity in responses to salinity. *Plant Physiology*, **166**, 1387–1402.

Lefebvre V., Fortabat M.N., Ducamp A., North H.M., Maia-Grondard A., Trouverie J., Boursiac Y., Mouille G., Durand-Tardif M. (2011) ESKIMO1 disruption in Arabidopsis alters vascular tissue and impairs water transport. *PLoS One*, **6**, e16645.

Líška D., Martinka M., Kohanová J., Lux A. (2016) Asymmetrical development of root endodermis and exodermis in reaction to abiotic stresses. *Annals of Botany*, **118**, 667–674.

Liu S.H., Fu B.Y., Xu H.X., Zhu L.H., Zhai H.Q., Li Z.K. (2007) Cell death in response to osmotic and salt stresses in two rice (*Oryza sativa* L.) ecotypes. *Plant Science*, **172**, 897–902.

Liu Y., Yu L., Qu Y., Chen J., Liu X., Hong H., Liu Z., Chang R., Gilliham M., Qiu L., Guan R. (2016) GmSALT3, which confers improved soybean salt tolerance in the field, increases leaf Cl^- exclusion prior to Na^+ exclusion but does not improve early vigor under salinity. *Frontiers in Plant Science*, **7**, 1–14.

Manchanda G., Garg N. (2008) Salinity and its effects on the functional biology of legumes. *Acta Physiologiae Plantarum*, **30**, 595–618.

Munns R., Tester M. (2008) Mechanisms of salinity tolerance. *Annual Review of Plant Biology*, **59**, 651–681.

Nishinari K., Fang Y., Guo S., Phillips G.O. (2014) Soy proteins: a review on composition, aggregation and emulsification. *Food Hydrocolloids*, **39**, 301–318.

Nja R.B., Merceron B., Faucher M., Fleurat-Lessard P., Béré E. (2018) NaCl – Changes stem morphology, anatomy and phloem structure in Lucerne (*Medicago sativa* cv. Gabès): Comparison of upper and lower internodes. *Micron*, **105**, 70–81.

O'Brien T.P., Feder N., McCully M.E. (1964) Polychromatic staining of plant cell walls by toluidine blue O. *Protoplasma*, **59**, 368–373.

Oliveira V.P., Lima M.D.R., Silva B.R.S., Batista B.L., Lobato A.K.S. (2019) Brassinosteroids confer tolerance to salt stress in *Eucalyptus urophylla* plants enhancing homeostasis, antioxidant metabolism and leaf anatomy. *Journal of Plant Growth Regulation*, **38**, 557–573.

Paniz F.P., Pedron T., Freire B.M., Torres D.P., Silva F.F., Batista B.L. (2018) Effective procedures for the determination of As, Cd, Cu, Fe, Hg, Mg, Mn, Ni, Pb, Se, Th, Zn, U and rare earth elements in plants and foodstuffs. *Analytical Methods*, **10**, 4094–4103.

Parihar P., Singh S., Singh R., Singh V.P., Prasad S.M. (2015) Effect of salinity stress on plants and its tolerance strategies: a review. *Environmental Science and Pollution Research*, **22**, 4056–4075.

Phang T.H., Shao G., Lam H.M. (2008) Salt tolerance in soybean. *Journal of Integrative Plant Biology*, **50**, 1196–1212.

Potters G., Pasternak T.P., Guisez Y., Palme K.J., Jansen M.A.K. (2007) Stress-induced morphogenic responses: growing out of trouble? *Trends in Plant Science*, **12**, 98–105.

Prince S.J., Murphy M., Mutava R.N., Durnell L.A., Valliyodan B., Grover S.J., Nguyen H.T. (2017) Root xylem plasticity to improve water use and yield in water-stressed soybean. *Journal of Experimental Botany*, **68**, 2027–2036.

Purushothaman R., Zaman-Allah M., Mallikarjuna N., Pannirselvam R., Krishnamurthy L., Gowda C.L.L. (2013) Root anatomical traits and their possible contribution to drought tolerance in grain legumes. *Plant Production Science*, **16**, 1–8.

Qin L., Kang W., Qi Y., Zhang Z., Wang N. (2016) The influence of silicon application on growth and photosynthesis response of salt stressed grapevines (*Vitis vinifera* L.). *Acta Physiologiae Plantarum*, **38**(68). https://doi.org/10.1007/s11738-016-2087-9

Risopatron J.P.M., Sun Y., Jones B.J. (2010) The vascular cambium: molecular control of cellular structure. *Protoplasma*, **247**, 145–161.

Robin A.H.K., Matthew C., Uddin M.J., Bayazid K.N. (2016) Salinity-induced reduction in root surface area and changes in major root and shoot traits at the phytomer level in wheat. *Journal of Experimental Botany*, **67**, 3719–3729.

Rodrigues C.R.F., Silva E.N., da Mata Moura R., dos Anjos D.C., Hernandez F.F.F., Viégas R.A. (2014) Physiological adjustment to salt stress in *R. communis* seedlings is associated with a probable mechanism of osmotic adjustment and a reduction in water lost by transpiration. *Industrial Crops and Products*, **54**, 233–239.

Sanjukta S., Rai A.K. (2016) Production of bioactive peptides during soybean fermentation and their potential health benefits. *Trends in Food Science & Technology*, **50**, 1–10.

Saqib M., Akhtar J., Qureshi R.H. (2005) Na^+ exclusion and salt resistance of wheat (*Triticum aestivum*) in saline-waterlogged conditions are improved by the development of adventitious nodal roots and cortical root aerenchyma. *Plant Science*, **169**, 125–130.

Sellami S., Le Hir R., Thorpe M.R., Aubry E., Wolff N., Vilaine F., Brini F., Dinant S. (2019) Arabidopsis natural accessions display adaptations in inflorescence growth and vascular anatomy to withstand high salinity during reproductive growth. *Plants*, **8**, 1–17.

Shen J., Xu G., Zheng H.Q. (2014) Apoplastic barrier development and water transport in *Zea mays* seedling roots under salt and osmotic stresses. *Protoplasma*, **252**, 173–180.

Shu K., Qi Y., Chen F., Meng Y., Luo X., Shuai H., Zhou W., Ding J., Du J., Liu J., Yang F., Wang Q., Liu W., Yong T., Wang X., Feng Y., Yang W. (2017) Salt stress represses soybean seed germination by negatively regulating GA biosynthesis while positively mediating ABA biosynthesis. *Frontiers in Plant Science*, **8**, 1–12.

Steel R.G., Torrie J.H., Dickey D.A. (2006) *Principles and procedures of statistics: a biometrical approach*, 3rd edn. McGraw-Hill, New York, USA.

Sun F., Zhang W., Hu H., Li B., Wang Y., Zhao Y., Li K., Liu M., Li X. (2008) Salt modulates gravity signaling pathway to regulate growth direction of primary roots in Arabidopsis. *Plant Physiology*, **146**, 178–188.

Sustr M., Soukup A., Tylova E. (2019) Potassium in root growth and development. *Plants*, **8**, 435.

Wang J., Li X., Liu Y., Zhao X. (2010) Salt stress induces programmed cell death in *Thellungiella halophila* suspension-cultured cells. *Journal of Plant Physiology*, **167**, 1145–1151.

Wang Y., Peng X., Salvato F., Wang Y., Yan X., Zhou Z., Lin J. (2019) Salt-adaptive strategies in oil seed crop *Ricinus communis* early seedlings (cotyledon vs. true leaf) revealed from proteomics analysis. *Ecotoxicology and Environmental Safety*, **171**, 12–25.

Yu X., Liang C., Chen J., Qi X., Liu Y., Li W. (2015) The effects of salinity stress on morphological characteristics, mineral nutrient accumulation and essential oil yield and composition in *Mentha canadensis* L. *Scientia Horticulturae*, **197**, 579–583.

Zahra J., Nazim H., Cai S., Han Y., Wu D., Zhang B., Haider S.I., Zhang G. (2014) The influence of salinity on cell ultrastructure and photosynthetic apparatus of barley genotypes differing in salt stress tolerance. *Acta Physiologiae Plantarum*, **36**, 1261–1269.

Zhang Y.-M., Ma H.-L., Calderón-Urrea A., Tian C.-X., Bai X.-M., Wei J.-M. (2016) Anatomical changes to protect organelle integrity account for tolerance to alkali and salt stresses in *Melilotus officinalis*. *Plant and Soil*, **406**, 327–340.

Zhu J.-K. (2002) Salt and drought stress signal transduction in plants. *Annual Review of Plant Biology*, **53**, 247–273.

Page title

Effect of progressive salt stress on growth, physiology, biochemistry and leaf structure of soybean plants

Breno Ricardo Serrão da Silva ● Bruno Lemos Batista ● Allan Klynger da Silva Lobato

B. R. S. Silva ● A. K. S. Lobato (✉)
Núcleo de Pesquisa Vegetal Básica e Aplicada, Universidade Federal Rural da Amazônia. Paragominas, Pará, Brazil.

B. L. Batista
Centro de Ciências Naturais e Humanas, Universidade Federal do ABC, Santo André, São Paulo, Brazil

e-mail: allanllobato@yahoo.com.br

Corresponding author: Allan Klynger da Silva Lobato
Mailing address: Rodovia PA 256, Paragominas, Pará, Brazil. Núcleo de Pesquisa Vegetal Básica e Aplicada, Universidade Federal Rural da Amazônia
Phone: +55-91-983089845
Fax: +55-91-983089845

Author contribution statement
AKSL was the advisor of this project, planning all phases of this research. BRSS conducted the experiment in the greenhouse and performed physiological, anatomical, biochemical and morphological determinations, while BLB performed nutritional determinations and helped in drafting the manuscript and in interpreting the results.

Data availability statement
Data are available upon request to the corresponding author.

Conflict of interest
The authors declare that they have no competing interests.

Effect of progressive salt stress on growth, physiology, biochemistry and leaf structure of soybean plants

Abstract

Soybean is a legume widely cultivated in several countries, mainly because the grains are rich in oil and proteins, where they are appreciated in human, animal food or in the production of consumer goods. On the other hand, one of the factors that limit global production is saline soils, where it is estimated that 800 million hectares of land are affected by salinity worldwide. Based on the hypothesis that the problems caused by saline stress promote responses and that the plant uses anatomical leaf changes to reduce excessive transpiration and consequently minimized the transport and accumulation of salt on the plant, the aim of this research was to evaluate the physiological, biochemical and nutritional parameters and how they influence the characteristic of soybean plants submitted to progressive salt stress. The experiment was conducted at random with five treatments (0, 50, 100, 150 and 200 mM NaCl). The data showed that in the highest concentrations of Na^+ negative interference in K^+/Na^+ homeostasis, nutritional content, photosynthetic apparatus and gas exchange, also the increase in oxidative damage and induced, to a certain extent, the antioxidant system and compromised the photosynthetic pigments. Structurally, it was observed in concentrations of up to 100 mM Na^+, greater deposition of epicuticular wax, changes in the amount and shape of the stomata and increased thickness of the leaf epidermis. Finally, our research showed that the effects caused by salinity promoted anatomical changes to minimize salt damage.

Keywords *Glycine max* ● Epicuticular wax ● Salinity

81 **Abbreviations**

APX	Ascorbate peroxidase
CAR	Carotenoids
CAT	Catalase
Chl *a*	Chlorophyll a
Chl *b*	Chlorophyll b
C_i	Intercellular CO_2 concentration
CO_2	Carbon dioxide
E	Transpiration rate
EDS	Equatorial diameter of the stomata
EL	Electrolyte leakage
ETAb	Epidermis thickness from abaxial leaf side
ETAd	Epidermis thickness from adaxial leaf side
ETR	Electron transport rate
ETR/P_N	Ratio between the apparent electron transport rate and net photosynthetic rate
EXC	Relative energy excess at the PSII level
EWL	Epicuticular wax load
F_0	Minimal fluorescence yield of the dark-adapted state
F_m	Maximal fluorescence yield of the dark-adapted state
F_v	Variable fluorescence
F_v/F_m	Maximal quantum yield of PSII photochemistry
g_s	Stomatal conductance
H_2O_2	Hydrogen peroxide
LDM	Leaf dry matter
LMD	Leaf metaxylem diameter
LPT	Leaf phoelm thickness
LXT	Leaf xylem thickness
MDA	Malondialdehyde
NPQ	Nonphotochemical quenching
O_2^-	Superoxide anion
PDS	Polar diameter of the stomata
P_N	Net photosynthetic rate
P_N/C_i	Instantaneous carboxylation efficiency
POX	Peroxidase
PPT	Palisade parenchyma thickness
PSII	Photosystem II

q_P	Photochemical quenching
RDM	Root dry matter
ROS	Reactive oxygen species
RuBisCO	Ribulose-1,5-bisphosphate carboxylase/oxygenase
SD	Stomatal density
SDM	Stem dry matter
SF	Stomatal functionality
SI	Stomatal index
SOD	Superoxide dismutase
SPT	Spongy parenchyma thickness
SPD	Stem pith diameter
SPhT	Stem phoelm thickness
SXT	Stem xylem thickness
TD	Trichome density
TDM	Total dry matter
Total Chl	Total Chlorophyll
TS	Trichome size
WUE	Water-use efficiency
Φ_{PSII}	Effective quantum yield of PSII photochemistry

Introduction

Soybean (*Glycine max* (L.) Merrill) is one of the most important crops in the world because grains are rich in oil and protein (Xu et al. 2016) which are appreciated in food and feed (Sanjukta and Rai 2016), besides being used as an energy source in biofuels (Pereira et al. 2017). Global production is estimated at approximately 338 million tons, with the United States being the main producer, followed by Brazil and Argentina (FAO 2018). However, one of the main factors limiting soy production is saline soils (Parihar et al. 2015), where approximately 800 million hectares of land are affected by salinity worldwide (FAO 2018).

Salinity is one of the main forms of abiotic stress, occurring mainly in arid and semi-arid regions, where it presents low precipitation and high evapotranspiration (Abuelgasim and Ammad 2019). However, anthropogenic factors may favor and potentiate salt accumulation through the use of low quality irrigation water, poorly drained soils, and overuse of fertilizers and pesticides (Manchanda and Garg 2008). Among the salts that are accumulated in soils and harmful to agricultural crops, NaCl stands out, which in recent years has been the target of numerous studies on its effects on plants (Shahbaz et al. 2011; Rasool et al. 2013; Qin et al. 2016b; de Oliveira et al. 2019).

The high concentrations of NaCl in the soil favors the accumulation of Na^+ ions inside the plant cell vacuoles (Horie et al. 2012) causing an osmotic imbalance by decreasing the soil water potential and reducing the plants ability to absorb water (Rengasamy 2010) and subsequently causing ionic imbalance, making Na^+ potentially toxic in plant metabolism (Blumwald 2000). This is due to the replacement of K^+ by Na^+ in cytosol, altering biochemical reactions and protein conformation, and K^+ acts as an enzymatic cofactor and protein synthesis (Zhu 2002). Furthermore, the osmotic pressure caused by excess Na^+ in the growth regions of the plant favors the competitive absorption between ions and hinders the locomotion and accumulation of macro and micronutrients essential for the plant (Parihar et al. 2015).

Plants under saline stress develop various strategies to tolerate saline stress to some extent, including morphological, physiological, biochemical and anatomical aspects, through alternative processes that include selective accumulation and / or exclusion of ions, control of the intake of root ions and leaf transport, compartmentalization of ions in the vacuoles and leaves, osmolytes synthesis, alteration of photosynthetic pathways and induction of antioxidant enzymes (Munns 2002; Acosta-Motos et al. 2017).

In mild to moderate Na^+ concentration, structural changes in the leaf epidermis are reported as a strategy to prevent direct solar radiation and excessive sweating through changes in the stomata guard cells (Barbieri et al. 2012), increased leaf hairiness (Bickford 2016) and epicuticular wax accumulation (Yang et al. 2015). On the other hand, under severe Na^+ exposure conditions oxidative stresses occur and negatively affect plant growth and development (Pulavarty et al. 2016), as well as increasing the accumulation of reactive oxygen species (ROS) and ionic toxicity, compromising the antioxidant defense mechanism, decreasing photosynthetic pigments and unbalancing hormones (Kim et al. 2016).

Our hypothesis was based on problems caused by saline stress on structural responses. Additionally, the anatomical modifications linked to leaves can contribute to the reduction of excessive transpiration and consequently minimize salt transport within the plant. The aim of this research was to

evaluate the physiological, biochemical and nutritional effects and how they affect the structural characteristics in soybean plants subjected to progressive salt stress.

Materials and Methods

Location and growth conditions

The experiment was performed at the Campus of Paragominas of the Universidade Federal Rural da Amazônia, Paragominas, Brazil (2°55' S, 47°34' W). The study was conducted in a greenhouse in which the temperature and humidity were controlled. The minimum, maximum and median temperatures were 24.6, 28.8 and 26.6 °C, respectively. The relative humidity during the experimental period varied between 60% and 80%.

Plants, containers and acclimation

Seeds of *Glycine max* (L.) Merr. var. M8644RR Monsoy™ were germinated and grown in 1.2-L pots filled with a mixed substrate of sand and vermiculite at a ratio of 3:1. The plants were cultivated under semi-hydroponic conditions containing 500 mL of distilled water for eight days. A modified Hoagland and Arnon (1950) solution was used for nutrients, with the ionic strength beginning at 50% (6th day) and later modified to 100% after two days (8th day). After this period, the nutritive solution remained at total ionic strength.

Experimental design

The experiment was randomized into five treatments (0, 50, 100, 150 and 200 mM NaCl, described as 0, 50, 100, 150 and 200 mM Na^+, respectively). Five replicates of each treatment were conducted, producing a total of 25 experimental units (pots), with one plant in each unit.

Plant conduction and salt stress

One plant per pot was used to examine the plant parameters. The plants received the following macro- and micronutrients in the nutrient solution: 8.75 mM KNO_3, 7.5 mM $Ca(NO_3)_2 \cdot 4H_2O$, 3.25 mM $NH_4H_2PO_4$, 1.5 mM $MgSO_4 \cdot 7\ H_2O$, 62.50 µM KCl, 31.25 µM H_3BO_3, 2.50 µM $MnSO_4 \cdot H_2O$, 2.50 µM $ZnSO_4 \cdot 7H_2O$, 0.63 µM $CuSO_4 \cdot 5H_2O$, 0.63 µM $NaMoO_4 \cdot 5H_2O$, and 250.0 µM $NaEDTAFe \cdot 3H_2O$. To simulate Na^+ exposure, NaCl was used at concentrations of 0, 50, 100, 150 and 200 mM Na, applied over 15 days (days 20–35 after the start of the experiment). During the study, the nutrient solutions were changed at 07:00 h at 3-day intervals, with the pH adjusted to 5.5 using HCl or NaOH. On day 35 of the experiment, physiological and morphological parameters were measured for all plants, and leaf tissues were harvested for anatomical, biochemical and nutritional analyses.

Measurement of chlorophyll fluorescence

The minimal fluorescence yield of the dark-adapted state (F_0), the maximal fluorescence yield of the dark-adapted state (F_m), the variable fluorescence (F_v), the maximal quantum yield of PSII photochemistry (F_v/F_m), the effective quantum yield of PSII photochemistry (Φ_{PSII}), the photochemical quenching coefficient (q_P), the nonphotochemical quenching (NPQ), the electron transport rate (ETR), the

relative energy excess at the PSII level (EXC) and the ratio between the electron transport rate and the net photosynthetic rate (ETR/P_N) were determined using a modulated chlorophyll fluorometer (model OS5p; Opti-Sciences). Chlorophyll fluorescence was measured in expanded leaves under light. Preliminary tests determined the location of the leaf, the part of the leaf and the time required to obtain the greatest F_v/F_m ratio. This evaluation used the acropetal third of leaves from in the middle third of the plant that were adapted to the dark for 30 min. The intensity and duration of the saturation light pulse were 7,500 μmol m^{-2} s^{-1} and 0.7 s, respectively.

Evaluation of gas exchange

The net photosynthetic rate (P_N), transpiration rate (E), stomatal conductance (g_s), and intercellular CO_2 concentration (C_i) were evaluated using an infrared gas analyser (model LCPro$^+$; ADC BioScientific). These parameters were measured in expanded leaves from middle region of the plant. The water-use efficiency (WUE) was estimated according to the protocol described by Ma et al. (2004), and the instantaneous carboxylation efficiency (P_N/C_i) was calculated using the formula described by Aragão et al. (2012). Gas exchange was evaluated in all plants under constant conditions. The CO_2 concentration was artificially controlled in 360 μmol mol^{-1} CO_2, photosynthetically active radiation was 800 μmol photons m^{-2} s^{-1}, the air-flow rate was 300 μmol s^{-1} and the temperature was 28 °C. Measurements were taken between 10:00 and 12:00 h

Measurements of anatomical parameters

Samples were collected from the middle region and midgrip of the leaf limb of fully expanded leaves. Subsequently, all collected botanical materials were fixed in FAA 70 for 24 hours and dehydrated in ethanol and embedded in Historesin Leica^{TM} (Leica, Nussloch, Germany). Transverse sections with a thickness of 5 μm were obtained using a rotating microtome (model Leica RM 2245, Leica Biosystems). The sections were stained with toluidine blue (O'Brien et al. 1964). The epidermal dissociation method was used for stomatal and trichome characterization. The slides were observed and photomicrographed under an optical microscope (Motic BA 310, Motic Group Co. LTD.) coupled to a digital camera (Motic 2500, Motic Group Co., LTD.). The images were analysed with a Moticplus 2.0 that had been previously calibrated with a micrometre slide from the manufacturer. The anatomical parameters evaluated were: the polar diameter of the stomata (PDS), the equatorial diameter of the stomata (EDS), the trichome size (TS), leaf metaxylem diameter (LMD), the leaf phoelm thickness (LPT), the leaf xylem thickness (LXT), the trichome density (TD) and the trichome size (TS), the epidermis thickness from adaxial leaf side (ETAd), the epidermis thickness from abaxial leaf side (ETAb), the palisade parenchyma thickness (PPT), the spongy parenchyma thickness (SPT). For both leaf faces, the stomatal density (SD) and trichome density (TD) was calculated as the number of stomata and trichome per unit area, respectivament, and the stomatal functionality (SF) was calculated as the ratio PDS/EDS, as described by Castro et al. (2009). The stomatal index (SI %) was calculated as the percentage of stomata in relation to total epidermal cells, by area.

Epicuticular wax quantification

Wax extraction was based on the recommendations of Damato et al. (2017) with modifications. In individual pre-weighed recipients, fragments 1 cm² of the middle third of the leaf were immersed in 2 mL chloroform for 30 seconds. The obtained extract was placed in a water bath at 60 °C until the total evaporation of chloroform and then weighed. Wax quantification was expressed by the amount of wax per unit leaf area (mg/cm^{-2}).

Extraction of antioxidant enzymes, superoxide anion and soluble proteins

Antioxidant enzymes (SOD, CAT, APX and POX), superoxide anion and soluble proteins were extracted from leaf tissues according to the method described by (Badawi et al. 2004). The extraction mixture was prepared by homogenizing 500 mg of fresh plant material in 5 ml of extraction buffer, which consisted of 50 mM phosphate buffer (pH 7.6), 1.0 mM ascorbate and 1.0 mM EDTA. Samples were centrifuged at 14,000 × *g* for 4 min at 3 °C, and the supernatant was collected. Quantification of the total soluble proteins was performed using the method described by (Bradford 1976). Absorbance was measured at 595 nm, using bovine albumin as a standard.

Superoxide dismutase assay

For the SOD assay (EC 1.15.1.1), 2.8 ml of a reaction mixture containing 50 mM phosphate buffer (pH 7.6), 0.1 mM EDTA, 13 mM methionine (pH 7.6), 75 µM NBT, and 4 µM riboflavin was mixed with 0.2 ml of supernatant. The absorbance was then measured at 560 nm (Giannopolitis and Ries 1977). One SOD unit was defined as the amount of enzyme required to inhibit 50% of the NBT photoreduction. The SOD activity was expressed in mg^{-1} protein.

Catalase assay

For the CAT assay (EC 1.11.1.6), 0.2 ml of supernatant and 1.8 ml of a reaction mixture containing 50 mM phosphate buffer (pH 7.0) and 12.5 mM hydrogen peroxide were mixed, and the absorbance was measured at 240 nm (Havir and McHale 1987). The CAT activity was expressed in µmol H_2O_2 mg^{-1} protein min^{-1}.

Ascorbate peroxidase assay

For the APX assay (EC 1.11.1.11), 1.8 ml of a reaction mixture containing 50 mM phosphate buffer (pH 7.0), 0.5 mM ascorbate, 0.1 mM EDTA, and 1.0 mM hydrogen peroxide was mixed with 0.2 ml of supernatant, and the absorbance was measured at 290 nm (Nakano and Asada 1981). The APX activity was expressed in µmol AsA mg^{-1} protein min^{-1}.

Peroxidase assay

For the POX assay (EC 1.11.1.7), 1.78 ml of a reaction mixture containing 50 mM phosphate buffer (pH 7.0) and 0.05% guaiacol was mixed with 0.2 ml of supernatant, followed by the addition of 20 µl of 10 mM hydrogen peroxide. Absorbance was then measured at 470 nm (Cakmak and Marschner 1992). POX activity was expressed in µmol tetraguaiacol mg^{-1} protein min^{-1}.

Determination of superoxide anion concentration

To determine the O_2^- concentration, 1 ml of extract was incubated with 30 mM phosphate buffer [pH 7.6] and 0.51 mM hydroxylamine hydrochloride for 20 min at 25 °C. Then, 17 mM sulphanilamide and 7 mM α-naphthylamine were added to the incubation mixture for 20 min at 25 °C. After the reaction, an identical volume of ethyl ether was added, and the mixture was centrifuged at 3,000 × *g* for 5 min. The absorbance was measured at 530 nm (Elstner and Heupel, 1976).

Extraction of oxidative stress markers

Oxidative stress markers (H_2O_2 and MDA) were extracted according to the protocol described by Wu et al. (2006). Briefly, a mixture of H_2O_2 and MDA was prepared by homogenizing 500 mg of fresh leaf materials in 5 ml of 5% (w/v) trichloroacetic acid. The samples were then centrifuged at 15,000 x g for 15 min at 3 °C, and the supernatant was collected.

Determination of hydrogen peroxide concentration

To measure H_2O_2, 200 µl of supernatant and 1800 µl of reaction mixture (2.5 mM potassium phosphate buffer [pH 7.0] and 500 mM potassium iodide) were mixed, and the absorbance was measured at 390 nm (Velikova et al. 2000).

Quantification of malondialdehyde concentration

MDA was measured by mixing 500 µl of supernatant with 1,000 µl of the reaction mixture, which contained 0.5% (w/v) thiobarbituric acid in 20% trichloroacetic acid. The mixture was incubated in boiling water at 95 °C for 20 min. The reaction was terminated by placing the reaction container in an ice bath. The samples were centrifuged at 10,000 × g for 10 min, and the absorbance was measured at 532 nm. The nonspecific absorption at 600 nm was subtracted from the absorbance data. The MDA–TBA complex (red pigment) amount was calculated based on the method of Cakmak and Horst (1991), with minor modifications and using an extinction coefficient of 155 mM^{-1} cm^{-1}.

Determination of electrolyte leakage

Electrolyte leakage was measured according to the method described by Gong et al. (1998), with minor modifications. Fresh tissue (200 mg) was cut into pieces that were 1 cm in length and placed in containers with 8 ml of distilled deionised water. The containers were incubated in a water bath at 40 °C for 30 min. The initial electrical conductivity of the medium (EC_1) was then measured. Next, the samples were boiled at 95 °C for 20 min to release the electrolytes. After cooling, their final electrical conductivity (EC_2) was measured (Gong et al. 1998). The percentage of electrolyte leakage was calculated using the formula EL (%) = (EC_1/EC_2) x 100.

Determination of photosynthetic pigments

The chlorophyll and carotenoid determinations were performed with 40 mg of leaf tissue. The samples were homogenized in the dark with 8 mL of 90% methanol (Nuclear). The homogenate was centrifuged at 6,000 × g for 10 min at 5°C. The supernatant was removed, and chlorophyll *a* (Chl *a*) and *b* (Chl *b*),

carotenoid (Car) and total chlorophyll (total Chl) contents were quantified using a spectrophotometer (model UV-M51; Bel Photonics), according to the methodology of Lichtenthaler and Buschmann (2001).

Determining of Na and nutrients

Samples with 100 mg of milled samples were weighed in 50-mL conical tubes (Falcon^R, Corning, Mexico) and pre-digested (48 h) with 2 ml of sub boiled HNO_3 (DST 1000, Savillex, USA). After, 8 ml of a solution containing 4 ml of H_2O_2 (30% v/v, Synth, Brasil) and 4 ml of ultra-pure water (Milli-Q System, Millipore, USA) were added, and the mixture was transferred to a Teflon digestion vessel, closed and heated in a block digester (EasyDigest®, Analab, France) according to the following program: i) 100°C for 30 min; ii) 150°C for 30 min; iii) 130°C for 10 min; iv) 100°C for 30 min and; and v) left to cool. The volume was made to 50 mL with ultra-pure water, and iridium was used as an internal standard at 10 µg l^{-1}. The determination of Na, K, P, Ca, Mg, S, Fe, Mn and Cu was carried out using an inductively coupled plasma mass spectrometer (ICP-MS 7900, Agilent, USA). Certified reference materials (NIST 1570a and NIST 1577c) were run in each batch for quality control purposes. All found values were in agreement with certified values.

Measurements of morphological parameters

The growth of roots, stems and leaves was measured based on constant dry weights (g) after drying in a forced-air ventilation oven at 65 °C.

Data analysis

The data were subjected to an analysis of variance, and significant differences between the means were determined using the Scott-Knott test at a probability level of 5% (Steel et al. 2006). Standard deviations were calculated for each treatment.

Results

Salinity reduced K^+ / Na^+ homeostasis and nutritional content

The addition of Na^+ in plants promoted influences ($P < 0.05$) on the content of Na^+, K^+ and K^+/ Na^+ of the leaves, showing increases of 453% to 86977% for Na^+, reductions of 6% to 29% for K^+ and 84% to 100% for K^+/Na^+, when compared to the control treatment (Table 1). The increase in salinity caused significant changes in nutritional content. Plants subjected to concentrations of 50 to 200 mM Na^+ had reductions that oscillated in Ca (38% to 63%), Mg (20% to 41%), S (14% to 27%), Fe (19% to 40%), Mn (10% to 28%) and Cu (13% to 37%), in relation to the control plants (Table 2).

Na^+ promoted damage in photosynthetic apparatus

Plants exposed to salinity exhibited significant increases in F_0 values, ranging of 14% to 37%, compared to control (Fig. 1). Differing of F_m, with continuous decreases of 3% to 23% as well as F_v of 8% to 40%. For F_v/F_m, salt stress induced significant losses that ranged of 5% to 22% in plants under concentrations of 50 to 200 mM Na^+, comparing with control plants. Plants subjected to concentrations of 50 to 200 mM Na^+ exhibited significant reductions in Φ_{PSII} (13% to 62%), q_P (1% to 30%) and ETR (13% to 62%)

(Table 3). On the other hand, salt stress caused increases of 32% to 141% for NPQ, of 8% to 52% for EXC and of 41% to 1472% for ETR/P_N, comparison with control treatment.

Salt stress affects gas exchange

Plants exposed to Na^+ had interferences (P<0.05) in gas exchange, P_N values ranging from 38% to 96%, in relation to the control (Table 4). Similar behaviors were observed in E, with decreases of 32% to 65%, as well as in g_s, with negative oscillations of 52% to 85%. Additionally, gradual reductions were detected in WUE (8% to 89%) and P_N/C_i (39% to 98%) in plants under 50 to 200 mM Na^+ concentrations, when compared to the control treatment.

Salinity interferes on stomata and trichomes

Plants submitted to 50 and 100 mM Na^+ presented significant increases, with peaks on the adaxial and abaxial faces in SD (44% and 23%), PDS (13% and 7%), EDS (29% and 17%), SF (15% and 15%) and SI (34% and 18%), in the same order, compared to the control plants (Table 5 and Fig. 2).

The increase in salinity caused impacts (P<0.05) on the trichomes on both faces, with damages more intense in the 200 mM Na^+ concentration. For TD, the reductions were 62% and 84%, while for TS 57% and 55% on the adaxial and abaxial faces, respectively, when compared to the control.

Modifications induced by the progressive salt stress on epicuticular wax and leaf structures

Salt stress promoted significant changes on EWL indices, with an increase of 12%, followed by reductions of 21%, 31% and 35% in plants under concentrations of 50, 100, 150 and 200 mM Na^+, respectively, if compared to control (Table 6). In SEM, it was possible to follow the behavior of EWL in leaf surface due to salt stress (Fig. 3). During the reduction of the wax deposition areas was verified that the losses occurred preferentially from the central region to the periphery of the epidermal cells. To leaf structures, plants subjected to Na^+ had significant effects (Table 6). The values of LXT, DVE, ETAd, ETAb and SPT under 100 mM Na^+ concentration increased by 28%, 6%, 62%, 46% and 57%, in this order, compared to control treatment, but under 200 mM Na^+ concentration reductions of 9%, 17%, 9%, 3% and 16% were detected, respectively. In LPT (50 mM Na^+), increases of 34% were observed, but with reductions of 12% under 200 mM Na^+ concentration. In relation to PPT, salinity caused significant increases that ranged from 12% to 54%, compared to the control treatment. Anatomically, the leaves of plants submitted to salinity presented the first alterations under 100 mM Na^+, when compared to the control (Fig. 4). In the central vein (in cross section), was observed progressive changes of the tissues, mainly of the vascular system, reduction of the the number, shape and size of the auxiliary bundles. Aditionally, also were detected spaces in the palisade parenchyma and minor arrangement of the spongy parenchyma of the leaf mesophyll.

Salinity modified the antioxidant system

Plants submitted to treatments with 50 to 200 mM Na^+ had significant increases in SOD levels (93% to 125%), compared to control (Fig. 5). On the other hand, salinity induced peaks in the activities of CAT, APX and POX enzymes under 100 mM Na^+ concentration, with significant interferences in CAT values

ranging from 5% to 121%, in POX ranging from 58% to 514% and APX ranging from 5% to 43%, if compared to the control.

Na^+ increases oxidative stress

Salinity caused significant interference in O_2^- values, with progressive increases of 2% to 40%. H_2O_2 had significant increases from 13% to 103% after salt stress (Fig. 6). For MDA, the values suffered significant increases of 8% to 30% in plants under concentrations of 50 to 200 mM Na^+. In relation to EL, salt stress caused significant interferences of 15% to 64% in plants under concentrations of 50 to 200 mM Na^+, when compared to the control.

Plants exposed to Na^+ toxicity decreases photosynthetic pigments

Saline conditions promoted changes ($P < 0.05$) on photosynthetic pigments, inducing reductions of 14% to 33% in Chl *a* values, and 18% to 69% in Chl *b*, compared to control, in plants under 50 to 200 mM Na^+ concentrations (Table 7). Similar trend was observed in the Total Chl, with losses ranging from 16% to 46% and in Car of 21% to 70%. However, plants subjected to 50 to 200 mM Na^+ presented progressive and significant increases in ratio Chl *a*/Chl *b* (16% to 46%) and ratio Total Chl/Car (21% to 70%), when compared to the control.

Salt stress negatively interferes on biomass

The biomass was significantly affected by the salt stress (Fig. 7 and Fig. 8). Plants exposed to Na^+ presented decreases of 36% to 76% for LDM, 43% to 75% for RDM, 51% to 78% for SDM, and 42% to 76% for TMD, when compared to control.

Discussion

The increases in Na^+ content in leaf tissues in plants confirm the effectiveness of salt stress in this study. High concentrations of salts, mainly Na^+, interfere with K^+ absorption due to the high affinity of transporters and also by non-selective cationic channels (Chen et al. 2005). This may justify the reduction in the K^+ content and the K^+/Na^+ ratio in the leaves with the increase in salinity. When there is an imbalance in the absorption of K^+, it causes several metabolic disorders in the plant, such as losses in enzymatic activation, protein synthesis, negative interferences in photosynthesis, cell expansion, stomatal movements, among others (Flowers et al. 2015). The accumulation of Na^+ in aerial organs, mainly in the leaf tissues, is a strategy to reduce the osmotic and ionic stress in the root tissues caused by this ion (Farooq et al. 2015). Silva et al. (2020), evaluating anatomical changes of stem and root of *Glycine max* submitted to progressive concentrations of 0 to 200 mM NaCl, observed a more accumulation of Na^+ in the aerial organ. Tiwari et al. (2010), submitting 17 genotypes of *Cucumis sativus* in four salinity levels, found increases in Na^+ content and decreases in K^+ accumulation and K^+/Na^+ ratio in the leaves of all analyzed genotypes. Ding et al. (2012), investigating the growth, the antioxidant system and the nutritional content in the leaves of *Solanus melongena* exposed to 90 mM NaCl, verified increases of 518% in the Na^+ content and decreases of 49% and 1022% in the accumulation of K^+ and relation K^+ / Na^+, respectively.

Plants submitted to salinity had reductions in the content of macronutrients (Ca, Mg and S) and micronutrients (Fe, Mn and Cu). These nutritional disorders are associated with high salt concentrations that increase osmotic pressure in the plants growth regions and interfere with the water and nutrient absorption capacity (Munns 2002). In this way, it favors the competitive absorption between ions and hinders the movement and accumulation of essential nutrients for the vegetable (Parihar et al. 2015).

Calcium is established as the second intracellular messenger in plants and its chemical by-products function as an important secondary messenger signaling molecule (Reddy et al. 2011). When the extracellular stress signal is perceived by membrane receptors, a complex cascade of intracellular signaling occurs, including Ca^{2+}, which favors the expression of multiple responsive stress genes and several responses to tolerance, such as reductions in plant growth, apoptosis, Na^+ translocation into the cells of older tissues, among others (Mahajan et al. 2008). On the other hand, the high Na^+ requirements can replace the Ca^{2+} of the membranes, leading to a decrease in the K^+/Na^+ selectivity (Munns and Tester 2008) and weakening a cell wall structure, making it more susceptible to ruptures (Hepler and Winship 2010). Reducing the concentration of K^+ and Ca^{2+} ions in tissues caused by salt stress is probably the main reason for the reduction in plant growth (Aghajanzadeh et al. 2019). Morgan et al. (2014) evaluating an ionic homeostasis and ATPase activities in *Vicia faba* submitted to 100 mM NaCl and in two harvest periods (7 and 14 days), found reductions in the content of Ca^{2+}. Similarly, Teixeira and Carvalho (2009), evaluating the saline influence (0, 60, 120 and 240 mM NaCl) on the mineral composition of *Portulaca oleracea*, observed reductions of up to 56% and 81% in the Ca content in plants sown in the spring and summer, respectively.

Similar as occurs in K^+ and Ca^{2+}, the decrease in Mg^{2+} in plant tissues under salinity conditions can happen due to Na interference (Mei et al. 2014). Mg belongs to the central structure of the Chl *a* molecule and participates in several enzymatic processes that involve phosphate transfer (Guo et al. 2015). The decrease in the Mg^{2+} content may also have contributed to the decrease in the photosynthetic pigment content observed in this study. Another nutrient that exhibit significant function in the formation of the photosynthetic apparatus and in the electron transport system is sulfur. The compounds containing S are also involved in ROS metabolism, in which they play an important role in mitigating salt-induced oxidative stress and improving K^+/Na^+ ion selectivity (Nazar et al. 2011). On the other hand, S deficiency obstructs plant metabolism, decreasing the chlorophyll content, photosynthetic efficiency and alters the content and activity of RuBisCO (Fatma et al. 2014). Bendaly et al. (2016) evaluating physiological and metabolomic changes of *Atriplex halimus* in progressive salinity from 0 to 400 mM NaCl, observed reductions in the Mg^{2+} contents in the higher salt concentrations. When studying the effect of 35 mM NaCl on the F6 cultivar of *Fragaria* × *ananassa*, Karlidag et al. (2011) found reductions of 75% and 47% in Mg and S contents, respectively.

In general, micronutrients act as a regulatory mechanism for Na uptake and translocation, in addition to being involved in the integrity and function of biomembranes in plants (El-Fouly et al. 2010). Fe is an important and essential micronutrient for the synthesis of chlorophyll and is present in plant enzymes that act in photosynthesis and cellular respiration (Xiong et al. 2014). Similarly, Mn also plays an important role as an activator of several enzymes, participates in photosynthesis, constitutes PSII proteins and activates decarboxylase, dehydrogenase, superoxidase and phosphatase (Schmidt and Husted

2019). Mn deficiency inhibits growth and induces chlorosis, necrosis and leaf fall (Schmidt et al. 2016). Cu is highly affected by salinity and the low absorption of this micronutrient can cause leaf damage as well as a significant reduction in chlorophyll pigments and photosynthesis, impairing the electron transport activity of PS II (Yruela 2009). When analyzing the nutritional content of *Cucumis sativus* plants submitted to salinity, Huang et al. (2010) found reductions of 69%, 73% and 65% in the amount of Fe, Mn and Cu, respectively. Oliveira et al. (2019) evaluating the morphological, physiological and biochemical impacts on the behavior of *Eucalyptus urophylla* seedlings exposed to 250 mM NaCl, found reduction of 59% reduction in Fe content.

The addition of Na^+ in the plants promoted successive increases in the F_0 values indicating that this ion decreased the proportion of oxidized quinone (Q_A) and negatively affected the efficiency of the capture of light energy in the PSII reaction center (Li et al. 2015). The reduction in the values of F_m, F_v and F_v/F_m observed after saline stress reveals a deficiency in the conversion of photochemical energy, with possible photoinhibition, or injuries caused in the PSII complex (Murchie and Lawson 2013). Additionally, salt stress impairs the structure and organization of the thylakoid membrane, often causing decreases in the photosynthetic activity of the reaction centers (Shu et al. 2013). Khoshbakht et al. (2018) evaluating the fluorescence parameters of chlorophyll in *Citrus reticulata* × *Citrus limetta* seedlings submitted to 75 mM NaCl found increases in F_0 values and reductions in F_m, F_v and F_v/F_m. Stepien and Johnson (2009) studying the photosynthetic responses of *Arabidopsis thaliana* found reductions in the values of F_v/F_m when submitting the plants in concentrations of 100 and 150 mM NaCl.

Plants exposed to concentrations of 50 to 200 mM Na + exhibited decreases in the values of Φ_{PSII}, q_P and ETR demonstrating less energy absorption from photons and subsequent decrease in energy flow for excitation of electrons captured by plastoquinone (Buonasera et al. 2011). On the other hand, the increase in the values of NPQ, EXC and ETR/P_N in plants with Na^+ suggests mechanisms of protection against damage in the PSII, such as greater thermal dissipation in the reaction center (Porcar-Castell et al. 2014) and increased photorespiration through the consumption of photochemical energy (Baker 2008). Yuan et al. (2014) evaluating photosynthetic performance and heat dissipation capacity in *Cucumbis sativus* plants submitted to 75 mM NaCl observed decreases of 35% and 35% in the values of Φ_{PSII} and q_P, respectively. Yan et al. (2014) investigating changes in photosynthesis and efficiency of PSII in leaves of *Caragana korshinskii* exposed to three levels of salinity (0, 100 and 300 mM NaCl) found increases in NPQ values and reductions in Φ_{PSII}, q_P and ETR after 1, 9 and 18 days after the application of stress. Aragão et al. (2012) submitting *Jatropha curcas* plants to levels of 0 and 100 mM NaCl detected decreases in the values of q_P and ETR of 28% and 36%, and increments in NPQ, EXC and ETR/P_N of 200%, 120% and 42%, in the same order.

Negative effects on P_N, E and gs were observed in plants exposed to salinity. The inadequate osmotic condition induced by the Na^+ stress probably stimulated the abscisic acid (ABA) biosynthesis, acting on stomatal closure and negatively influencing on gs values (Acosta-Motos et al. 2017). Additionally, stomatal-related limitations, as evidenced by reductions in SD, SI and SF, impair E and CO_2 influx, inducing reductions in P_N (Hasanuzzaman et al. 2018). In other words, the reductions of E and P_N, coupled with the low performance in stomatal regulation (g_s) justify the reduction detected in WUE and clear limitations on gas exchange. Agrawal et al. (2013) evaluating the growth, gas exchange and ionic

regulation of two *Ziziphus mauritiana* cultivars submitted to NaCl (electrical conductivity from 0 to 16 dS m^{-1}) observed decreases in P_N, *gs* and *E* values. Equivalent physiological responses to our research were found by Zheng et al. (2009) comparing the performance of two *Triticum aestivum* genotypes exposed to 50, 100 and 150 mM Na^+, describing reductions in P_N and *gs*. Shahbaz et al. (2011)evaluating the repercussions of the salt stress on growth, photosynthetic capacity and ion accumulation in eight *Helianthus annuus* cultivars found reductions in WUE.

The increases showed on P_N/C_i in plants under concentrations of 50 to 200 mM Na^+ indicates a decrease in RuBisCO enzyme activity, compromising CO_2 fixation in the Calvin-Benson cycle and resulting in an increase in C_i (He et al. 2014). Rodrigues et al. (2014) evaluating the physiological adjustment of *Ricinus communis* plants under concentrations of 50, 100 and 150 mM NaCl reported increases in P_N/C_i values. Chen et al. (2009) observed increases in C_i after comparing the progressive effects of the salinity (40 to 200 mM NaCl) on growth and photosynthetic attributes of *Populus bonatii* cultivars.

In relation to SD and SI were observed partial increases in concentrations of 50 and 100 mM Na^+, being explained by the decrease of the epidermal cell expansion and leaf area (Fu et al. 2013). On the other hand, decreases in SD and SI (150 and 200 mM NaCl) negatively affected the CO_2 absorption and consequently the g_s values (Asmar et al. 2013). The oscillations in the numbers of PDS, EDS and SF proved that the salt stress structurally influenced the stomata, inducing an elliptic form. Khan et al. (2003) described that elliptical stomata have better functionality, when compared with the circular form. The decreases in TS and TD values (50 to 200 mM Na^+) were linked to two effects simultaneous, the salt stress and higher sun exposure on epidermal cells, favoring water losses via transpiration process (Bickford 2016b). Barbieri et al. (2012) comparing two *Ocimun basilicum* cultivars under concentrations of 100 and 200 mM NaCl showed reductions in SD values. Sarabi et al. (2017) studying *Cucumis melo* plants submitted to 30, 60 and 90 mM Na^+ verified successive decreases on TS and TD values.

The partial increase in EWL observed at 50 mM NaCl is essential to improve the radiation reflection incident on the epidermis, protecting against excessive transpiration and respiration, consequently decreasing the leaf temperature (Sheperd and Griffiths 2006). However, under concentrations higher than 100 mM NaCl there is a degradation of epicuticular wax that may be correlated with Na^+ and Cl^- accumulations in leaves (Yang et al. 2015). Avestan et al. (2019) studying *Fragaria ananassa* (25 and 50 mM NaCl) observed changes in structure and reduction in the amount of EWL.

Anatomical changes in vascular bundles and the reduction in LXT and LPT values observed under 200 mM Na^+ clearly affected the solute translocation by the conductive tissues and reduced the photoassimilate accumulation (Nikinmaa et al. 2013). On ETAd and ETAb in plants exposed up to 100 mM Na^+, the partial increases suggest an anatomical adaptation to salinity, aiming to prevent the excessive water loss during transpiration (Javelle et al. 2011). On the other hand, the reduction in these leaf anatomical variables may indicate that plants under concentrations above 150 mM NaCl are in susceptible to damages caused by severe salinity. The decreases in PPT and SPT (200 mM Na^+) may have contributed to the decrease in P_N, C_i and P_N/C_i values, because the palisade parenchyma presents the largest amount of chloroplasts, being these organelles responsible for the photosynthetic process, while

SPT is related to intense formation of intercellular spaces involved with gas exchange (Sorin et al. 2015). Moreover, the large arrangement found in the mesophyll impairs the cell surface contact and consequently the capture of light energy and gas exchange necessary during the photosynthetic process (Polizel et al. 2011). Paz et al. (2014) submitting *Lotus tenuis* plants in solution containing 90 mM NaCl found increases in ETAd, ETAb, PPT and SPT values.

Plants exposed to salinity (> 50 mM Na^+) had increases in SOD, CAT, APX and POX activities, demonstrating the efficiency of the antioxidant system in relation ROS accumulation under simulated saline stress in this research. SOD catalyzes the reaction of O_2^- forming H_2O_2 (Gill and Tuteja 2010), while CAT, APX and POX convert H_2O_2 to non-reactive compounds, such as H_2O and O_2 (Abedi and Pakniyat 2010). Fariduddin et al. (2013) found increases in SOD and CAT activities assessing the activities of the antioxidant enzymes in two *Cucumis sativus* cultivars exposed to 150 mM Na^+. El-Mashad and Mohamed (2012) investigating the salinity effects on antioxidant system found increases in POX activities after *Vigna sinensis* plants subjected to 100 and 150 mM NaCl. Rasool et al. (2013) using growth parameters and biochemical attributes in eight *Cicer arietinum* genotypes under concentrations of 25 to 100 mM NaCl, reported increases in SOD, CAT, and APX enzymes.

Increases in MDA and EL values found in plants exposed to Na^+ clearly reveal damages on membranes caused by the action of ROS, such as O_2^- and H_2O_2. ROS are highly reactive and toxic, causing structural and functional deteriorations of the membranes and subsequent lipid peroxidation (Yuan et al. 2010; Siddiqui et al. 2015). Increases in MDA, EL and H_2O_2 were observed by Hu et al. (2012) studying genes, proteins and enzymes linked to antioxidant metabolism in two *Lolium perenne* genotypes under 250 mM NaCl. Farhangi-Abriz and Torabian (2017) evaluating antioxidant enzymes, oxidative stress and osmotic adjustment in *Phaseolus vulgaris* seedlings submitted to three levels of salinity (0, 6 and 12 dSm^{-1} NaCl), found increases in MDA, O_2^- and H_2O_2.

Damages on photosynthetic pigments (Chl *a*, Chl *b*, Total Chl and Car) in plants exposed to salt stress is associated with oxidative stress promoted by increases in MDA, O_2^- and H_2O_2 previously detected in this study. These substances are highly toxic and promote the degradation of the thylakoid membranes, where there is a high concentration of chlorophyll molecules, and negatively interfere with the biosynthesis of these pigments (Takahashi and Badger 2011). Shu et al. (2012) evaluating the effects of the saline stress (75 mM NaCl) on the structures and functions of photosynthetic apparatus in *Cucumis sativus* plants found reductions in Chl *a*, Chl *b* and Total Chl values. Similar behavior was observed by Ma et al. (2012) evaluating *Oryza sativa* leaves submitted to 150 mM NaCl obtaining decreases of 21%, 19% and 20% in Chl *a*, Chl *b* and Total Chl, respectively. Aghaleh et al. (2009) studying the progressive effects of the salt stress (100 to 600 mM NaCl) in two species of the *Salicornia* genus detected reductions in Chl *a*, Chl *b* and Car contents in both species.

Salinity affected the plant growth, promoting reductions in LDM, RDM, SDM and TDM values. The lower biomass in plants exposed to Na^+ can be explained by multiple effects, such as reductions in stomatal characteristics, gas exchange and chlorophyll fluorescence. Under salt stress conditions often there is a reduction in biomass, because the osmotic stress caused by the Na^+ negatively affects the processes linked to cell division and elongation (Fricke and Peters 2002; Munns and Tester 2008). This ion also inhibits the root system development due to structural and functional restrictions, with

consequent impacts on nutrient uptake and translocation (Zahra et al. 2014), besides reductions in light and CO_2 capture and inefficient stomatal regulation (Degl'Innocenti et al. 2009; Hussain et al. 2016). Qin et al. (2016) observed decreases in LDM, RDM and SDM values submitting *Vitis vinifera* plants under salt conditions. Khan et al. (2014) investigating the physiological and biochemical behavior in *Vigna radiata* plants exposed to salt stress (100 mM NaCl) found reductions in TDM.

Conclusion

This research has shown that progressive salt stress interferes negatively in K^+/Na^+ homeostasis, nutritional content, photosynthetic apparatus and gas exchange, also increases oxidative damage and to some extent induces the antioxidant system and impairs photosynthetic pigments. On the other hand, salinity impacts promote leaf anatomical modifications to minimize the deleterious effects linked to Na^+. Effects such as the increase of epicuticular wax under saline concentrations of 50 mM Na^+ favor a lipophilic protection that avoids the loss of water by perspiration and the direct incidence of solar radiation on epidermal cells. Additionally, the improvements observed in stomata quantity, in their most elliptical shape, as well as the increase of epidermis thickness, up to 100 mM Na^+, evidences a strategy for the efficient use of water.

Acknowledgements

This research had financial supports from Fundação Amazônia de Amparo a Estudos e Pesquisas (FAPESPA/Brazil), Conselho Nacional de Desenvolvimento Científico e Tecnológico (CNPq/Brazil) and Universidade Federal Rural da Amazônia (UFRA/Brazil) to AKSL. In other hand, BRSS was supported with scholarship from Coordenação de Aperfeiçoamento de Pessoal de Nível Superior (CAPES/Brazil).

References

Abedi T, Pakniyat H (2010) Antioxidant enzymes changes in response to drought stress in ten cultivars of oilseed rape (Brassica napus L.). Czech J Genet Plant Breed 46:27–34. https://doi.org/10.17221/67/2009-CJGPB

Abuelgasim A, Ammad R (2019) Mapping soil salinity in arid and semi-arid regions using Landsat 8 OLI satellite data. Remote Sens Appl Soc Environ 13:415–425. https://doi.org/10.1016/j.rsase.2018.12.010

Acosta-Motos JR, Ortuño MF, Bernal-Vicente A, et al (2017) Plant responses to salt stress: Adaptive mechanisms. Agronomy 7:1–38. https://doi.org/10.3390/agronomy7010018

Aghajanzadeh TA, Reich M, Hawkesford MJ, Burow M (2019) Sulfur metabolism in Allium cepa is hardly affected by chloride and sulfate salinity. Arch Agron Soil Sci 65:945–956. https://doi.org/10.1080/03650340.2018.1540037

Aghaleh M, Niknam V, Ebrahimzadeh H, Razavi K (2009) Salt stress effects on growth, pigments, proteins and lipid peroxidation in Salicornia persica and S. europaea. Biol Plant 53:243–248. https://doi.org/10.1007/s10535-009-0046-7

Agrawal R, Gupta S, Gupta NK, et al (2013) Effect of sodium chloride on gas exchange, antioxidative defense mechanism and ion accumulation in different cultivars of Indian jujube (Ziziphus

620 mauritiana L.). Photosynthetica 51:95–101. https://doi.org/10.1007/s11099-013-0003-8
621 Aragão RM, Silva EN, Vieira CF, Silveira JAG (2012) High supply of NO3 − mitigates salinity effects
622 through an enhancement in the efficiency of photosystem II and CO2 assimilation in Jatropha
623 curcas plants. Acta Physiol Plant 34:2135–2143. https://doi.org/10.1007/s11738-012-1014-y
624 Asmar SA, Castro EM, Pasqual M, et al (2013) Changes in leaf anatomy and photosynthesis of
625 micropropagated banana plantlets under different silicon sources. Sci Hortic (Amsterdam) 161:328–
626 332. https://doi.org/10.1016/j.scienta.2013.07.021
627 Avestan S, Ghasemnezhad M, Esfahani M, Byrt CS (2019) Application of nano-silicon dioxide improves
628 salt stress tolerance in strawberry plants. Agronomy 9:1–17.
629 https://doi.org/10.3390/agronomy9050246
630 Badawi GH, Yamauchi Y, Shimada E, et al (2004) Enhanced tolerance to salt stress and water deficit by
631 overexpressing superoxide dismutase in tobacco (Nicotiana tabacum) chloroplasts. Plant Sci
632 166:919–928. https://doi.org/10.1016/j.plantsci.2003.12.007
633 Baker NR (2008) Chlorophyll fluorescence: a probe of photosynthesis in vivo. Annu Rev Plant Biol
634 59:89–113. https://doi.org/10.1146/annurev.arplant.59.032607.092759
635 Barbieri G, Vallone S, Orsini F, et al (2012) Stomatal density and metabolic determinants mediate salt
636 stress adaptation and water use efficiency in basil (Ocimum basilicum L.). J Plant Physiol
637 169:1737–1746. https://doi.org/10.1016/j.jplph.2012.07.001
638 Bendaly A, Messedi D, Smaoui A, et al (2016) Physiological and leaf metabolome changes in the
639 xerohalophyte species Atriplex halimus induced by salinity. Plant Physiol Biochem 103:208–218.
640 https://doi.org/10.1016/j.plaphy.2016.02.037
641 Bickford CP (2016a) Ecophysiology of leaf trichomes. Funct Plant Biol 43:807–814.
642 https://doi.org/10.1071/FP16095
643 Bickford CP (2016b) Ecophysiology of leaf trichomes. Funct Plant Biol 43:807.
644 https://doi.org/10.1071/FP16095
645 Blumwald E (2000) Sodium transport and salt tolerance in plants. Curr Opin Cell Biol 12:431–434.
646 https://doi.org/10.1016/S0955-0674(00)00112-5
647 Bradford MM (1976) A rapid and sensitive method for the quantitation of microgram quantities of protein
648 utilizing the principle of protein-dye binding. Anal Biochem 72:248–254.
649 https://doi.org/10.1016/0003-2697(76)90527-3
650 Buonasera K, Lambreva M, Rea G, et al (2011) Technological applications of chlorophyll a fluorescence
651 for the assessment of environmental pollutants. Anal Bioanal Chem 401:1139–1151.
652 https://doi.org/10.1007/s00216-011-5166-1
653 Cakmak I, Horst WJ (1991) Effect of aluminium on lipid peroxidation, superoxide dismutase, catalase,
654 and peroxidase activities in root tips of soybean (Glycine max). Physiol Plant 83:463–468.
655 https://doi.org/10.1111/j.1399-3054.1991.tb00121.x
656 Cakmak I, Marschner H (1992) Magnesium deficiency and high light intensity enhance activities of
657 superoxide dismutase, ascorbate peroxidase, and glutathione reductase in bean leaves. Plant Physiol
658 98:1222–1227. https://doi.org/10.1104/pp.98.4.1222
659 Castro EM, Pereira FJ, Paiva R (2009) Plant histology: Structure and function of vegetative organs. 234

660 Chen W, Zou D, Guo W, et al (2009) Effects of salt stress on growth, photosynthesis and solute
661 accumulation in three poplar cultivars. Photosynthetica 47:415–421.
662 https://doi.org/10.1007/s11099-009-0063-y
663 Chen Z, Newman I, Zhou M, et al (2005) Screening plants for salt tolerance by measuring K+ flux: a case
664 study for barley. Plant, Cell Environ 28:1230–1246. https://doi.org/10.1111/j.1365-
665 3040.2005.01364.x
666 de Oliveira VP, Lima MDR, da Silva BRS, et al (2019) Brassinosteroids Confer Tolerance to Salt Stress
667 in Eucalyptus urophylla Plants Enhancing Homeostasis, Antioxidant Metabolism and Leaf
668 Anatomy. J Plant Growth Regul 38:557–573. https://doi.org/10.1007/s00344-018-9870-3
669 Degl'Innocenti E, Hafsi C, Guidi L, Navari-Izzo F (2009) The effect of salinity on photosynthetic activity
670 in potassium-deficient barley species. J Plant Physiol 166:1968–1981.
671 https://doi.org/10.1016/j.jplph.2009.06.013
672 Ding HD, Zhu X-H, Zhu ZW, et al (2012) Amelioration of salt-induced oxidative stress in eggplant by
673 application of 24-epibrassinolide. Biol Plant 56:767–770. https://doi.org/10.1007/s10535-012-0108-
674 0
675 El-Fouly MM, Mobarak ZM, Salama ZA (2010) Improving Tolerance of Faba Bean during Early Growth
676 Stages to Salinity through Micronutrients Foliar Spray. Not Sci Biol 2:98–102.
677 https://doi.org/10.15835/nsb223701
678 El-Mashad AAA, Mohamed HI (2012) Brassinolide alleviates salt stress and increases antioxidant
679 activity of cowpea plants (Vigna sinensis). Protoplasma 249:625–635.
680 https://doi.org/10.1007/s00709-011-0300-7
681 Elstner EF, Heupel A (1976) Inhibition of nitrite formation from hydroxylammoniumchloride: A simple
682 assay for superoxide dismutase. Anal Biochem 70:616–620. https://doi.org/10.1016/0003-
683 2697(76)90488-7
684 Farhangi-Abriz S, Torabian S (2017) Antioxidant enzyme and osmotic adjustment changes in bean
685 seedlings as affected by biochar under salt stress. Ecotoxicol Environ Saf 137:64–70.
686 https://doi.org/10.1016/j.ecoenv.2016.11.029
687 Fariduddin Q, Khalil RRAE, Mir BA, et al (2013) 24-Epibrassinolide regulates photosynthesis,
688 antioxidant enzyme activities and proline content of Cucumis sativus under salt and/or copper
689 stress. Environ Monit Assess 185:7845–7856. https://doi.org/10.1007/s10661-013-3139-x
690 Farooq M, Hussain M, Wakeel A, Siddique KHM (2015) Salt stress in maize: effects, resistance
691 mechanisms, and management. A review. Agron Sustain Dev 35:461–481.
692 https://doi.org/10.1007/s13593-015-0287-0
693 Fatma M, Asgher M, Masood A, Khan NA (2014) Excess sulfur supplementation improves
694 photosynthesis and growth in mustard under salt stress through increased production of glutathione.
695 Environ Exp Bot 107:55–63. https://doi.org/10.1016/j.envexpbot.2014.05.008
696 Flowers TJ, Munns R, Colmer TD (2015) Sodium chloride toxicity and the cellular basis of salt tolerance
697 in halophytes. Ann Bot 115:419–431. https://doi.org/10.1093/aob/mcu217
698 Fricke W, Peters WS (2002) The biophysics of leaf growth in salt-stressed Barley. A study at the cell
699 level. Plant Physiol 129:374–388. https://doi.org/10.1104/pp.001164

700 Fu QS, Yang RC, Wang HS, et al (2013) Leaf morphological and ultrastructural performance of eggplant
701 (Solanum melongena L.) in response to water stress. Photosynthetica 51:109–114.
702 https://doi.org/10.1007/s11099-013-0005-6
703 Giannopolitis CN, Ries SK (1977) Superoxide dismutases: I. occurrence in higher plants. Plant Physiol
704 59:309–314
705 Gill SS, Tuteja N (2010) Reactive oxygen species and antioxidant machinery in abiotic stress tolerance in
706 crop plants. Plant Physiol Biochem 48:909–930. https://doi.org/10.1016/j.plaphy.2010.08.016
707 Gong M, Li Y-J, Chen S-Z (1998) Abscisic acid-induced thermotolerance in maize seedlings is mediated
708 by calcium and associated with antioxidant systems. J Plant Physiol 153:488–496.
709 https://doi.org/10.1016/S0176-1617(98)80179-X
710 Guo W, Chen S, Hussain N, et al (2015) Magnesium stress signaling in plant: Just a beginning. Plant
711 Signal Behav 10:37–41. https://doi.org/10.4161/15592324.2014.992287
712 Hasanuzzaman M, Shabala L, Zhou M, et al (2018) Factors determining stomatal and non-stomatal
713 (residual) transpiration and their contribution towards salinity tolerance in contrasting barley
714 genotypes. Environ Exp Bot 153:10–20. https://doi.org/10.1016/j.envexpbot.2018.05.002
715 Havir EA, McHale NA (1987) Biochemical and developmental characterization of multiple forms of
716 catalase in tobacco leaves. Plant Physiol 84:450–455. https://doi.org/10.1104/pp.84.2.450
717 He Y, Yu C, Zhou L, et al (2014) Rubisco decrease is involved in chloroplast protrusion and Rubisco-
718 containing body formation in soybean (Glycine max.) under salt stress. Plant Physiol Biochem
719 74:118–124. https://doi.org/10.1016/j.plaphy.2013.11.008
720 Hepler PK, Winship LJ (2010) Calcium at the cell wall-cytoplast interface. J Integr Plant Biol 52:147–60.
721 https://doi.org/10.1111/j.1744-7909.2010.00923.x
722 Hoagland DR, Arnon DI (1950) The water-culture method for growing plants without soil, 2nd edn.
723 California Agricultural Experiment Station
724 Horie T, Karahara I, Katsuhara M (2012) Salinity tolerance mechanisms in glycophytes: An overview
725 with the central focus on rice plants. Rice 5:1–18. https://doi.org/10.1186/1939-8433-5-11
726 Hu L, Li H, Pang H, Fu J (2012) Responses of antioxidant gene, protein and enzymes to salinity stress in
727 two genotypes of perennial ryegrass (Lolium perenne) differing in salt tolerance. J Plant Physiol
728 169:146–156. https://doi.org/10.1016/j.jplph.2011.08.020
729 Huang Y, Bie Z, He S, et al (2010) Improving cucumber tolerance to major nutrients induced salinity by
730 grafting onto Cucurbita ficifolia. Environ Exp Bot 69:32–38.
731 https://doi.org/10.1016/j.envexpbot.2010.02.002
732 Hussain MI, Lyra DA, Farooq M, et al (2016) Salt and drought stresses in safflower: a review. Agron
733 Sustain Dev 36:1–31. https://doi.org/10.1007/s13593-015-0344-8
734 Javelle M, Vernoud V, Rogowsky PM, Ingram GC (2011) Epidermis: The formation and functions of a
735 fundamental plant tissue. New Phytol 189:17–39. https://doi.org/10.1111/j.1469-8137.2010.03514.x
736 Karlidag H, Yildirim E, Turan M (2011) Role of 24-epibrassinolide in mitigating the adverse effects of
737 salt stress on stomatal conductance, membrane permeability, and leaf water content, ionic
738 composition in salt stressed strawberry (Fragaria×ananassa). Sci Hortic (Amsterdam) 130:133–140.
739 https://doi.org/10.1016/j.scienta.2011.06.025

740 Khan MIR, Asgher M, Khan NA (2014) Alleviation of salt-induced photosynthesis and growth inhibition
741 by salicylic acid involves glycinebetaine and ethylene in mungbean (Vigna radiata L.). Plant
742 Physiol Biochem 80:67–74. https://doi.org/10.1016/j.plaphy.2014.03.026
743 Khan PSSV, Kozai T, Nguyen QT, et al (2003) Growth and water relations of Paulownia fortunei under
744 photomixotrophic and photoautrophic conditions. Biol Plant 46:161–166.
745 https://doi.org/10.1023/A:1022844720795
746 Khoshbakht D, Asghari MR, Haghighi M (2018) Influence of foliar application of polyamines on growth,
747 gas-exchange characteristics, and chlorophyll fluorescence in Bakraii citrus under saline conditions.
748 Photosynthetica 56:731–742. https://doi.org/10.1007/s11099-017-0723-2
749 Kim J, Liu Y, Zhang X, et al (2016) Analysis of salt-induced physiological and proline changes in 46
750 switchgrass (Panicum virgatum) lines indicates multiple response modes. Plant Physiol Biochem
751 105:203–212. https://doi.org/10.1016/j.plaphy.2016.04.020
752 Li J, Yang P, Gan Y, et al (2015) Brassinosteroid alleviates chilling-induced oxidative stress in pepper by
753 enhancing antioxidation systems and maintenance of photosystem II. Acta Physiol Plant 37:1–11.
754 https://doi.org/10.1007/s11738-015-1966-9
755 Lichtenthaler HK, Buschmann C (2001) Chlorophylls and carotenoids: Measurement and characterization
756 by UV-VIS spectroscopy. In: Current Protocols in Food Analytical Chemistry. John Wiley & Sons,
757 Inc., Hoboken, NJ, USA, pp 431–438
758 Ma JF, Mitani N, Nagao S, et al (2004) Characterization of the silicon uptake system and molecular
759 mapping of the silicon transporter gene in rice. Plant Physiol 136:3284–3289.
760 https://doi.org/10.1104/pp.104.047365
761 Ma L, Li Y, Yu C, et al (2012) Alleviation of exogenous oligochitosan on wheat seedlings growth under
762 salt stress. Protoplasma 249:393–399. https://doi.org/10.1007/s00709-011-0290-5
763 Mahajan S, Pandey GK, Tuteja N (2008) Calcium- and salt-stress signaling in plants: shedding light on
764 SOS pathway. Arch Biochem Biophys 471:146–158. https://doi.org/10.1016/j.abb.2008.01.010
765 Manchanda G, Garg N (2008) Salinity and its effects on the functional biology of legumes. Acta Physiol
766 Plant 30:595–618. https://doi.org/10.1007/s11738-008-0173-3
767 Mei XQ, Li SS, Li QS, et al (2014) Sodium chloride salinity reduces Cd uptake by edible amaranth
768 (Amaranthus mangostanus L.) via competition for Ca channels. Ecotoxicol Environ Saf 105:59–64.
769 https://doi.org/10.1016/j.ecoenv.2014.04.005
770 Morgan SH, Maity PJ, Geilfus CM, et al (2014) Leaf ion homeostasis and plasma membrane H+-ATPase
771 activity in Vicia faba change after extra calcium and potassium supply under salinity. Plant Physiol
772 Biochem 82:244–253. https://doi.org/10.1016/j.plaphy.2014.06.010
773 Munns R (2002) Comparative physiology of salt and water stress. Plant, Cell Environ 25:239–250.
774 https://doi.org/10.1046/j.0016-8025.2001.00808.x
775 Munns R, Tester M (2008) Mechanisms of Salinity Tolerance. Annu Rev Plant Biol 59:651–681.
776 https://doi.org/10.1146/annurev.arplant.59.032607.092911
777 Murchie EH, Lawson T (2013) Chlorophyll fluorescence analysis: A guide to good practice and
778 understanding some new applications. J Exp Bot 64:3983–3998. https://doi.org/10.1093/jxb/ert208
779 Nakano Y, Asada K (1981) Hydrogen peroxide is scavenged by ascorbate-specific peroxidase in spinach

780 chloroplasts. Plant Cell Physiol 22:867–880
781 Nazar R, Iqbal N, Masood A, et al (2011) Understanding the significance of sulfur in improving salinity
782 tolerance in plants. Environ Exp Bot 70:80–87. https://doi.org/10.1016/j.envexpbot.2010.09.011
783 Nikinmaa E, Hölttä T, Hari P, et al (2013) Assimilate transport in phloem sets conditions for leaf gas
784 exchange. Plant, Cell Environ 36:655–669. https://doi.org/10.1111/pce.12004
785 O'Brien TP, Feder N, McCully ME (1964) Polychromatic staining of plant cell walls by toluidine blue O.
786 Protoplasma 59:368–373. https://doi.org/10.1007/BF01248568
787 Parihar P, Singh S, Singh R, et al (2015) Effect of salinity stress on plants and its tolerance strategies: a
788 review. Environ Sci Pollut Res 22:4056–4075. https://doi.org/10.1007/s11356-014-3739-1
789 Paz RC, Reinoso H, Espasandin FD, et al (2014) Akaline, saline and mixed saline-alkaline stresses induce
790 physiological and morpho-anatomical changes in Lotus tenuis shoots. Plant Biol 16:1042–1049.
791 https://doi.org/10.1111/plb.12156
792 Pereira GG, Garcia RKA, Ferreira LL, Barrera-Arellano D (2017) Soybean and soybean/beef-tallow
793 biodiesel: a comparative study on oxidative degradation during long-term storage. J Am Oil Chem
794 Soc 94:587–593. https://doi.org/10.1007/s11746-017-2962-6
795 Polizel AM, Medri ME, Nakashima K, et al (2011) Molecular, anatomical and physiological properties of
796 a genetically modified soybean line transformed with rd29A: AtDREB1A for the improvement of
797 drought tolerance. Genet Mol Res 10:3641–3656.
798 https://doi.org/http://dx.doi.org/10.4238/2011.October.21.4 ABSTRACT.
799 Porcar-Castell A, Tyystjärvi E, Atherton J, et al (2014) Linking chlorophyll a fluorescence to
800 photosynthesis for remote sensing applications: mechanisms and challenges. J Exp Bot 65:4065–
801 4095. https://doi.org/10.1093/jxb/eru191
802 Pulavarty A, Kukde S, Shinde VM, Sarangi BK (2016) Morphological, physiological and biochemical
803 adaptations of Eucalyptus citriodora seedlings under NaCl stress in hydroponic conditions. Acta
804 Physiol Plant 38:1–12. https://doi.org/10.1007/s11738-015-2042-1
805 Qin L, Kang W huai, Qi Y ling, et al (2016a) The influence of silicon application on growth and
806 photosynthesis response of salt stressed grapevines (Vitis vinifera L.). Acta Physiol Plant 38:1–9.
807 https://doi.org/10.1007/s11738-016-2087-9
808 Qin L, Kang W, Qi Y, et al (2016b) The influence of silicon application on growth and photosynthesis
809 response of salt stressed grapevines (Vitis vinifera L.). Acta Physiol Plant 38:68.
810 https://doi.org/10.1007/s11738-016-2087-9
811 Rasool S, Ahmad A, Siddiqi TO, Ahmad P (2013) Changes in growth, lipid peroxidation and some key
812 antioxidant enzymes in chickpea genotypes under salt stress. Acta Physiol Plant 35:1039–1050.
813 https://doi.org/10.1007/s11738-012-1142-4
814 Reddy ASN, Ali GS, Celesnik H, Day IS (2011) Coping with stresses: Roles of calcium- and
815 calcium/calmodulin-regulated gene expression. Plant Cell 23:2010–2032.
816 https://doi.org/10.1105/tpc.111.084988
817 Rengasamy P (2010) Soil processes affecting crop production in salt-affected soils. Funct Plant Biol
818 37:613–620. https://doi.org/10.1071/FP09249
819 Rodrigues CRF, Silva EN, da Mata Moura R, et al (2014) Physiological adjustment to salt stress in R.

communis seedlings is associated with a probable mechanism of osmotic adjustment and a reduction in water lost by transpiration. Ind Crops Prod 54:233–239. https://doi.org/10.1016/j.indcrop.2013.12.041

Sanjukta S, Rai AK (2016) Production of bioactive peptides during soybean fermentation and their potential health benefits. Trends Food Sci Technol 50:1–10. https://doi.org/10.1016/j.tifs.2016.01.010

Sarabi B, Bolandnazar S, Ghaderi N, Ghashghaie J (2017) Genotypic differences in physiological and biochemical responses to salinity stress in melon (Cucumis melo L.) plants: Prospects for selection of salt tolerant landraces. Plant Physiol Biochem 119:294–311. https://doi.org/10.1016/j.plaphy.2017.09.006

Schmidt SB, Husted S (2019) The biochemical properties of manganese in plants. Plants 8:. https://doi.org/10.3390/plants8100381

Schmidt SB, Jensen PE, Husted S (2016) Manganese deficiency in plants: The impact on photosystem II. Trends Plant Sci 21:622–632. https://doi.org/10.1016/j.tplants.2016.03.001

Shahbaz M, Ashraf M, Akram NA, et al (2011) Salt-induced modulation in growth, photosynthetic capacity, proline content and ion accumulation in sunflower (Helianthus annuus L.). Acta Physiol Plant 33:1113–1122. https://doi.org/10.1007/s11738-010-0639-y

Sheperd T, Griffiths DW (2006) The effects of stress on plant cuticular waxes. New Phytol 171:469–499

Shu S, Guo SR, Sun J, Yuan LY (2012) Effects of salt stress on the structure and function of the photosynthetic apparatus in Cucumis sativus and its protection by exogenous putrescine. Physiol Plant 146:285–296. https://doi.org/10.1111/j.1399-3054.2012.01623.x

Shu S, Yuan L-Y, Guo S, et al (2013) Effects of exogenous spermine on chlorophyll fluorescence, antioxidant system and ultrastructure of chloroplasts in Cucumis sativus L. under salt stress. Plant Physiol Biochem 63:209–216. https://doi.org/10.1016/j.plaphy.2012.11.028

Siddiqui MH, Al-Khaishany MY, Al-Qutami MA, et al (2015) Response of different genotypes of faba bean plant to drought stress. Int J Mol Sci 16:10214–10227. https://doi.org/10.3390/ijms160510214

Silva BRS, Batista BL, da Silva Lobato AK (2020) Anatomical changes in stem and root of soybean plants submitted to salt stress. Plant Biol plb.13176. https://doi.org/10.1111/plb.13176

Sorin C, Musse M, Mariette F, et al (2015) Assessment of nutrient remobilization through structural changes of palisade and spongy parenchyma in oilseed rape leaves during senescence. Planta 241:333–346. https://doi.org/10.1007/s00425-014-2182-3

Steel RG., Torrie JH, Dickey DA (2006) Principles and procedures of statistics: a biometrical approach, 3rd edn. Academic Internet Publishers, Moorpark

Stepien P, Johnson GN (2009) Contrasting responses of photosynthesis to salt stress in the Glycophyte Arabidopsis and the Halophyte Thellungiella: role of the plastid terminal oxidase as an alternative electron sink. Plant Physiol 149:1154–1165. https://doi.org/10.1104/pp.108.132407

Takahashi S, Badger MR (2011) Photoprotection in plants: A new light on photosystem II damage. Trends Plant Sci 16:53–60. https://doi.org/10.1016/j.tplants.2010.10.001

Teixeira M, Carvalho IS (2009) Effects of salt stress on purslane (Portulaca oleracea) nutrition. Ann Appl Biol 154:77–86. https://doi.org/10.1111/j.1744-7348.2008.00272.x

Tiwari JK, Munshi AD, Kumar R, et al (2010) Effect of salt stress on cucumber: Na+ -K+ ratio, osmolyte concentration, phenols and chlorophyll content. Acta Physiol Plant 32:103–114. https://doi.org/10.1007/s11738-009-0385-1

Velikova V, Yordanov I, Edreva A (2000) Oxidative stress and some antioxidant systems in acid rain-treated bean plants protective role of exogenous polyamines. Plant Sci 151:59–66. https://doi.org/10.1016/S0168-9452(99)00197-1

Wu Q-S, Xia R-X, Zou Y-N (2006) Reactive oxygen metabolism in mycorrhizal and non-mycorrhizal citrus (Poncirus trifoliata) seedlings subjected to water stress. J Plant Physiol 163:1101–1110. https://doi.org/10.1016/j.jplph.2005.09.001

Xiong H, Guo X, Kobayashi T, et al (2014) Expression of peanut Iron regulated transporter 1 in tobacco and rice plants confers improved iron nutrition. Plant Physiol Biochem 80:83–89. https://doi.org/10.1016/j.plaphy.2014.03.021

Xu D, Zhang J, Cao Y, et al (2016) Influence of microcrystalline cellulose on the microrheological property and freeze-thaw stability of soybean protein hydrolysate stabilized curcumin emulsion. LWT - Food Sci Technol 66:590–597. https://doi.org/10.1016/j.lwt.2015.11.002

Yan H, Hu X, Li F (2014) Leaf photosynthesis, chlorophyll fluorescence, ion content and free amino acids in Caragana korshinskii Kom exposed to NaCl stress. Acta Physiol Plant 36:2285–2295. https://doi.org/10.1007/s11738-012-1029-4

Yang C, Ma S, Lee I, et al (2015) Saline-induced changes of epicuticular waxy layer on the Puccinellia tenuiflora and Oryza sativa leave surfaces. Biol Res 48:1–8. https://doi.org/10.1186/s40659-015-0023-x

Yruela I (2009) Copper in plants: Acquisition, transport and interactions. Funct Plant Biol 36:409–430. https://doi.org/10.1071/FP08288

Yuan GF, Jia CG, Li Z, et al (2010) Effect of brassinosteroids on drought resistance and abscisic acid concentration in tomato under water stress. Sci Hortic (Amsterdam) 126:103–108. https://doi.org/10.1016/j.scienta.2010.06.014

Yuan Y, Shu S, Li S, et al (2014) Effects of exogenous putrescine on chlorophyll fluorescence imaging and heat dissipation capacity in cucumber (Cucumis sativus L.) under salt stress. J Plant Growth Regul 33:798–808. https://doi.org/10.1007/s00344-014-9427-z

Zahra J, Nazim H, Cai S, et al (2014) The influence of salinity on cell ultrastructures and photosynthetic apparatus of barley genotypes differing in salt stress tolerance. Acta Physiol Plant 36:1261–1269. https://doi.org/10.1007/s11738-014-1506-z

Zheng YH, Xu XB, Wang MY, et al (2009) Responses of salt-tolerant and intolerant wheat genotypes to sodium chloride: Photosynthesis, antioxidants activities, and yield. Photosynthetica 47:87–94. https://doi.org/10.1007/s11099-009-0014-7

Zhu J-K (2002) Salt and drought stress signal transduction in plants. Annu Rev Plant Biol 53:247–273. https://doi.org/10.1146/annurev.arplant.53.091401.143329

Figures

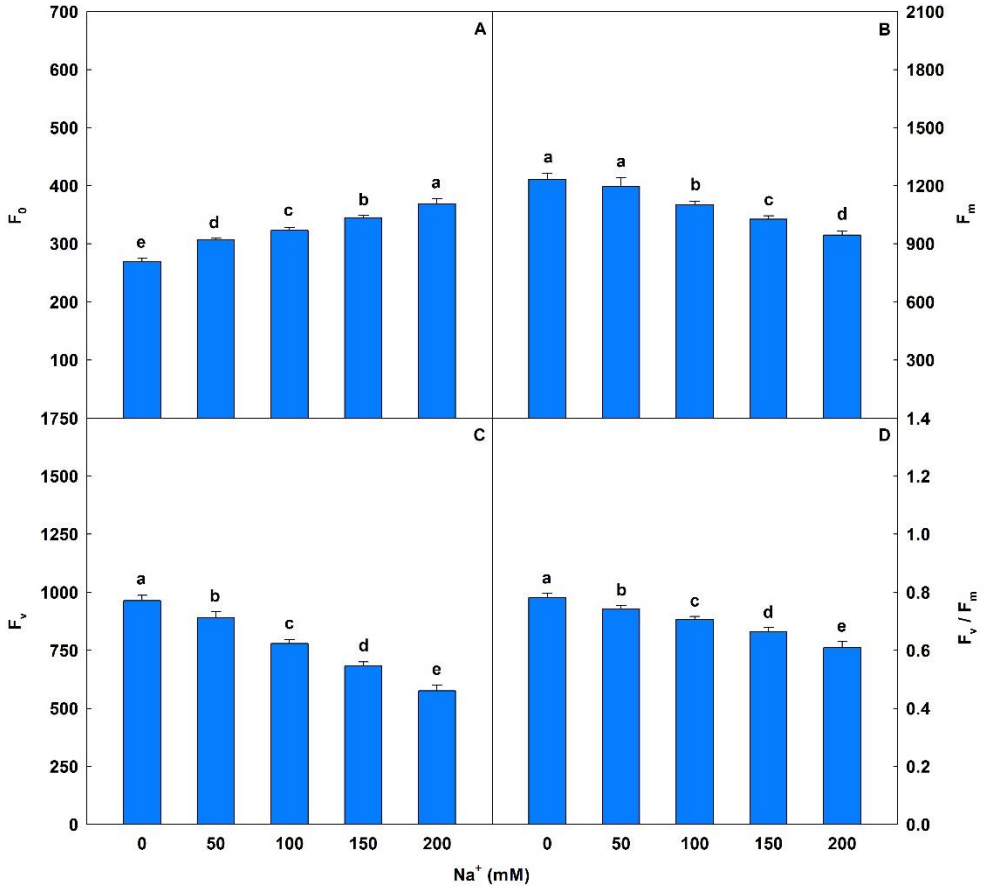

Fig. 1. Minimal fluorescence yield of the dark-adapted state (F_0), maximal fluorescence yield of the dark-adapted state (F_m), variable fluorescence (F_v) and maximal quantum yield of PSII photochemistry (F_v/F_m) in soybean plants submitted to salt stress. Bars with different letters indicate significant differences from the Scott-Knott test ($P<0.05$). Bars corresponding to means from five repetitions and standard deviations.

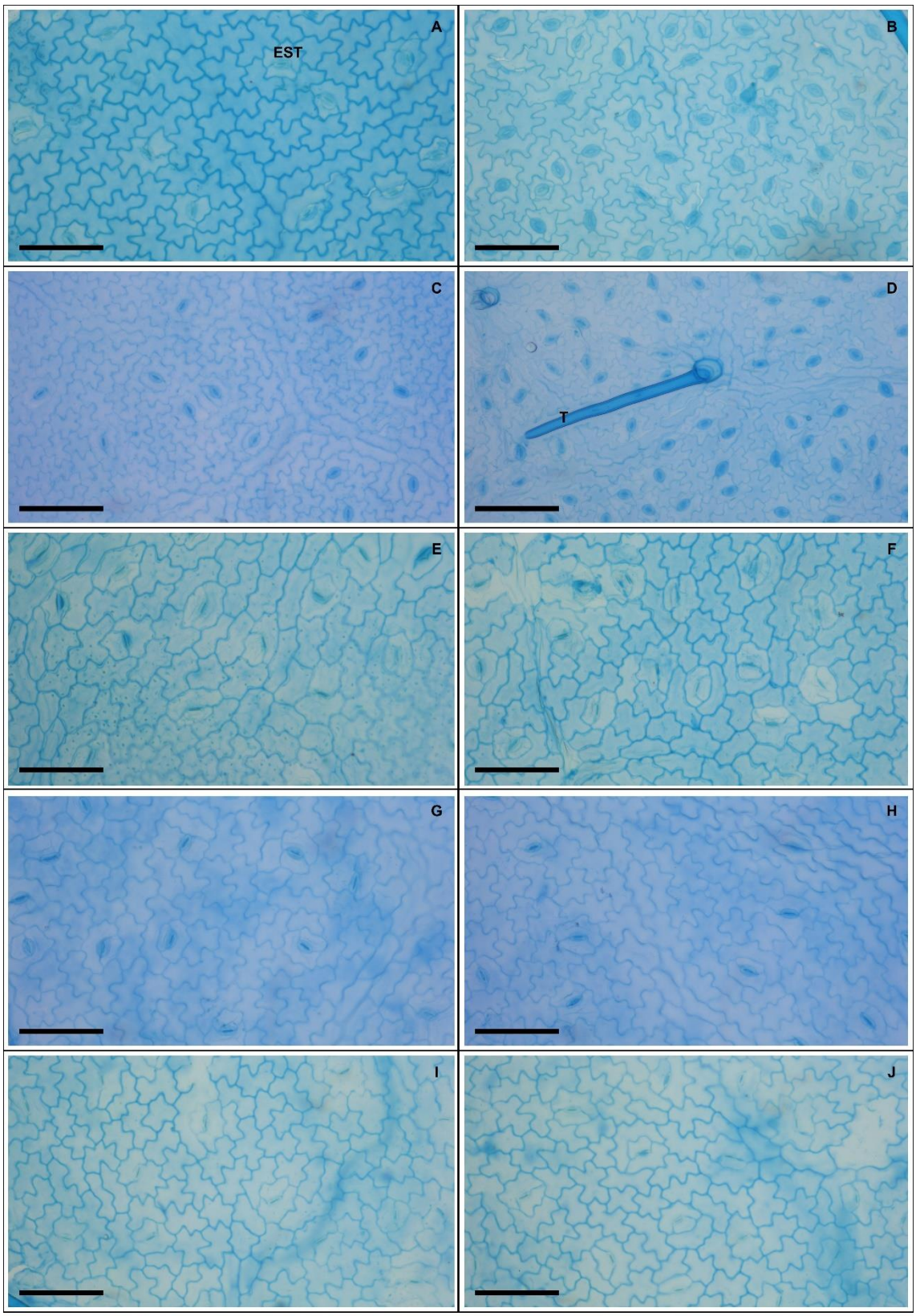

Fig. 2. Adaxial leaf surface (A, C, E, G and I) and abaxial (B, D, F, H and J) in soybean plants submitted to salt stress. 0 mM Na^+ (A – B), 50 mM Na^+ (C – D), 100 mM Na^+ (E – F), 150 mM Na^+ (G – H) and 200 mM Na^+ (I – J). Legends: EST = Stomata, T = Trichome. Bars: 50 µm.

927

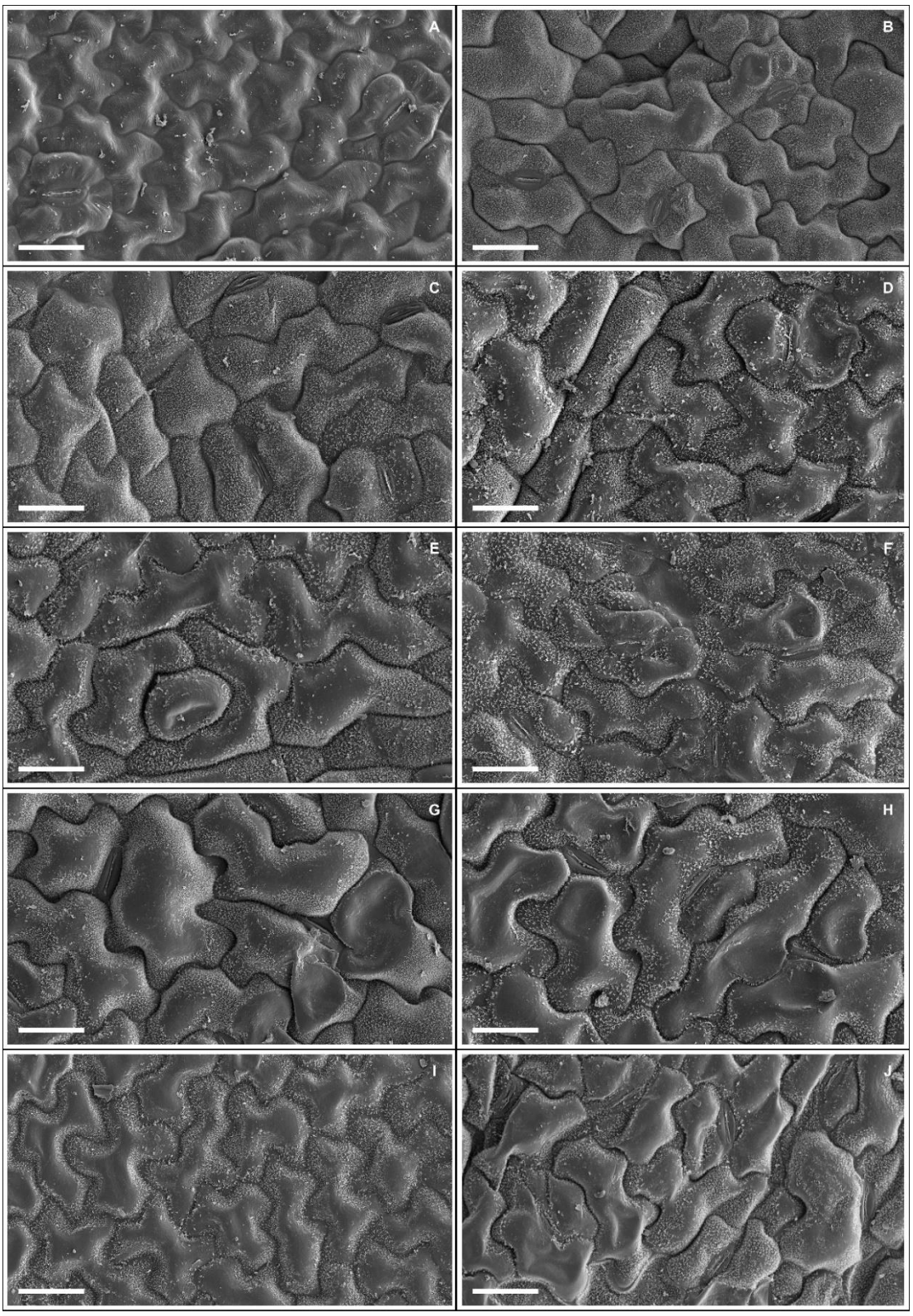

928

929 Fig. 3. Adaxial leaf surface (A, C, E, G and I) and abaxial (B, D, F, H and J) in scanning electron
930 microscopy showing epicuticular wax deposits in soybean plants submitted to salt stress. 0 mM Na^+ (A –
931 B), 50 mM Na^+ (C – D), 100 mM Na^+ (E – F), 150 mM Na^+ (G – H) and 200 mM Na^+ (I – J). Bars: 25
932 µm.

933

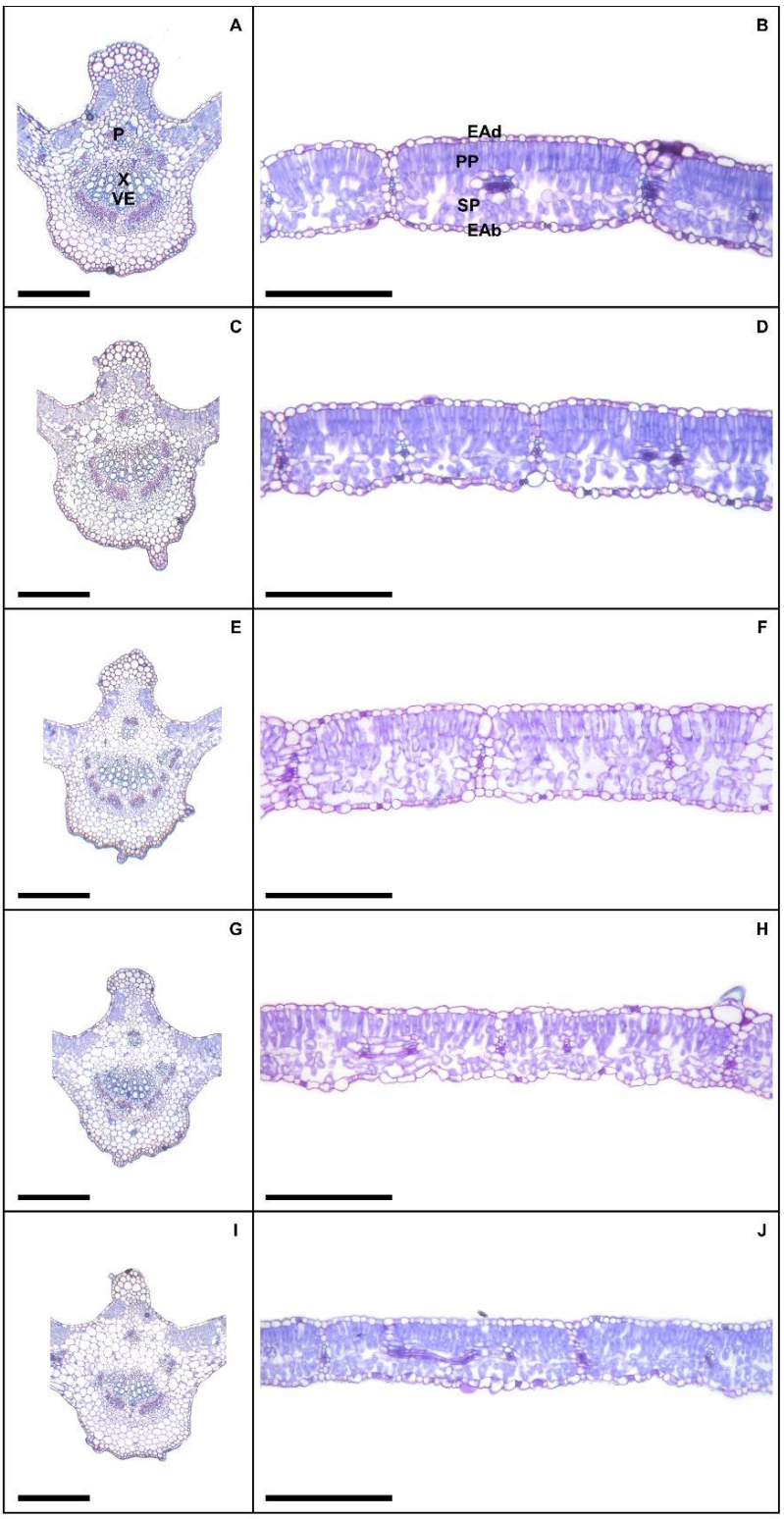

Fig. 4. Leaf cross section showing midrib (A, C, E, G and I) and the middle region (B, D, F, H and J) in soybean plants submitted to salt stress. Legends: 0 mM Na^+ (A – B), 50 mM Na^+ (C – D), 100 mM Na^+ (E – F), 150 mM Na^+ (G – H) and 200 mM Na^+ (I – J). Legends: P = Phoelm, X = Xylem, VE = vessel elements, EAd = Adaxial epidermis, EAb = Abaxial epidermis, PP = Palisade parenchyma, SP = Spongy parenchyna. Bars: 150 µm.

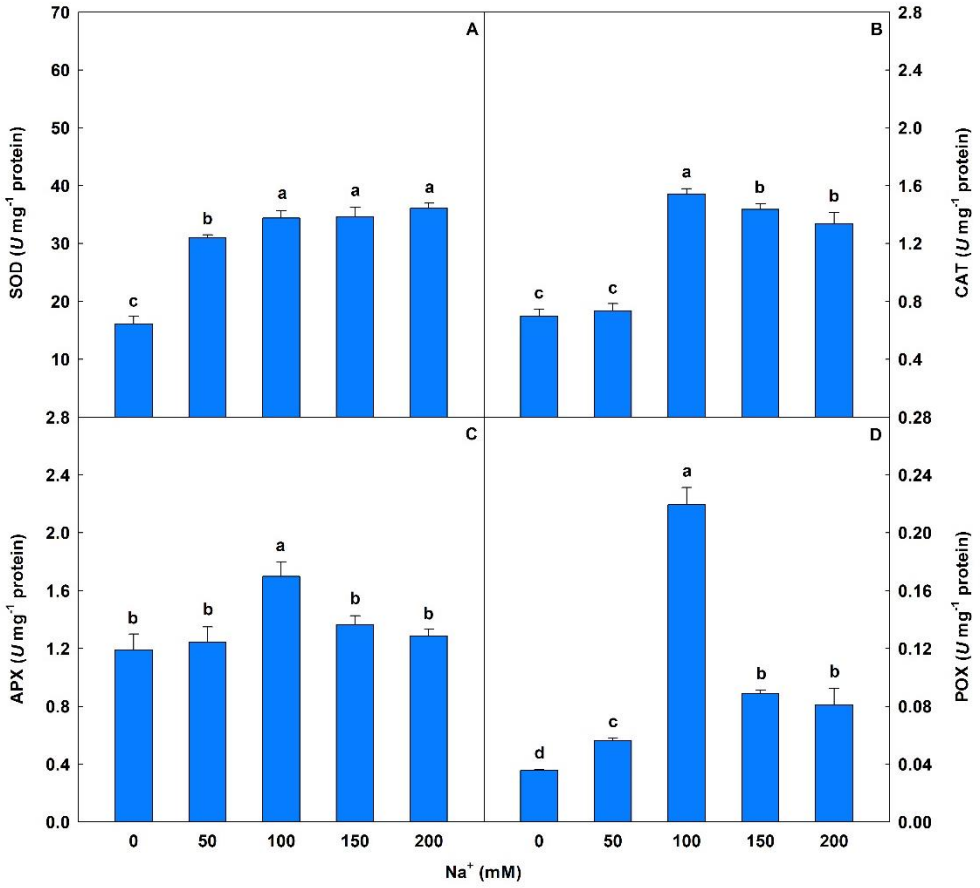

Fig. 5. Activities of superoxide dismutase (SOD), catalase (CAT), ascorbate peroxidase (APX) and peroxidase (POX) in soybean plants submitted to salt stress. Bars with different letters indicate significant differences from the Scott-Knott test (P<0.05). Bars corresponding to means from five repetitions and standard deviations.

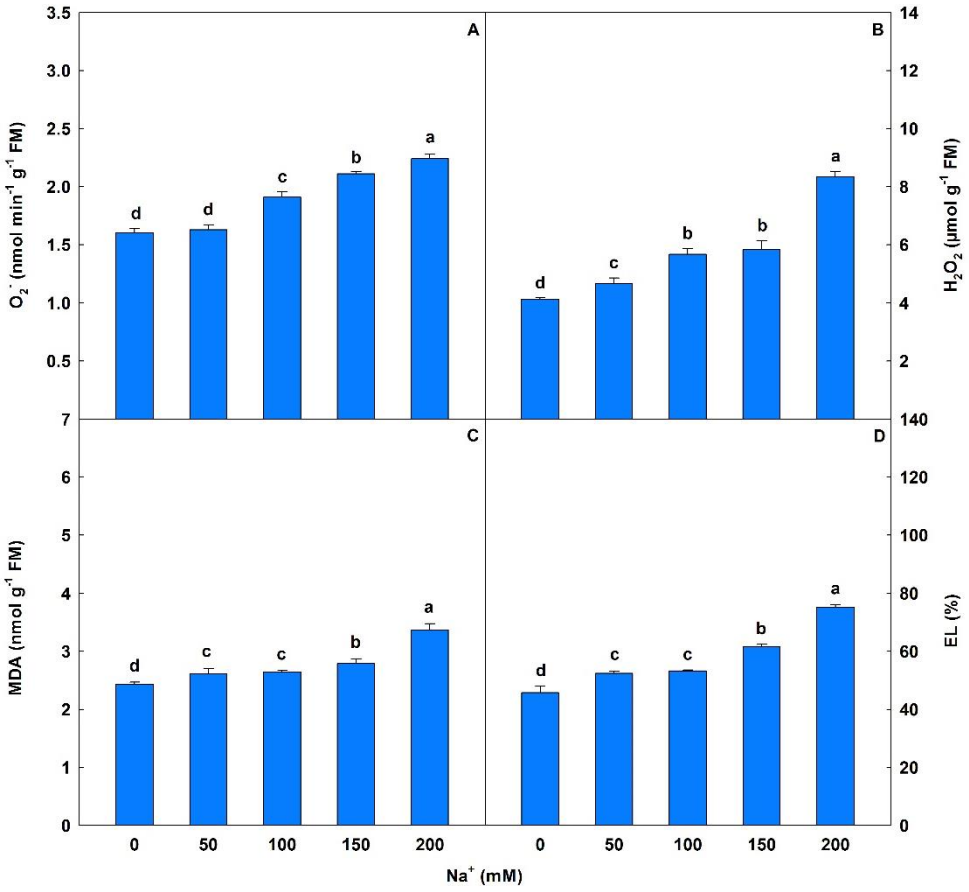

Fig. 6. Superoxide anion ($O_2^{\cdot-}$), hydrogen peroxide (H_2O_2), malondialdehyde (MDA) and electrolyte leakage (EL) in soybean plants sprayed with EBR and exposed to salt stress. Bars with different letters indicate significant differences from the Scott-Knott test (P<0.05). Bars corresponding to means from five repetitions and standard deviations.

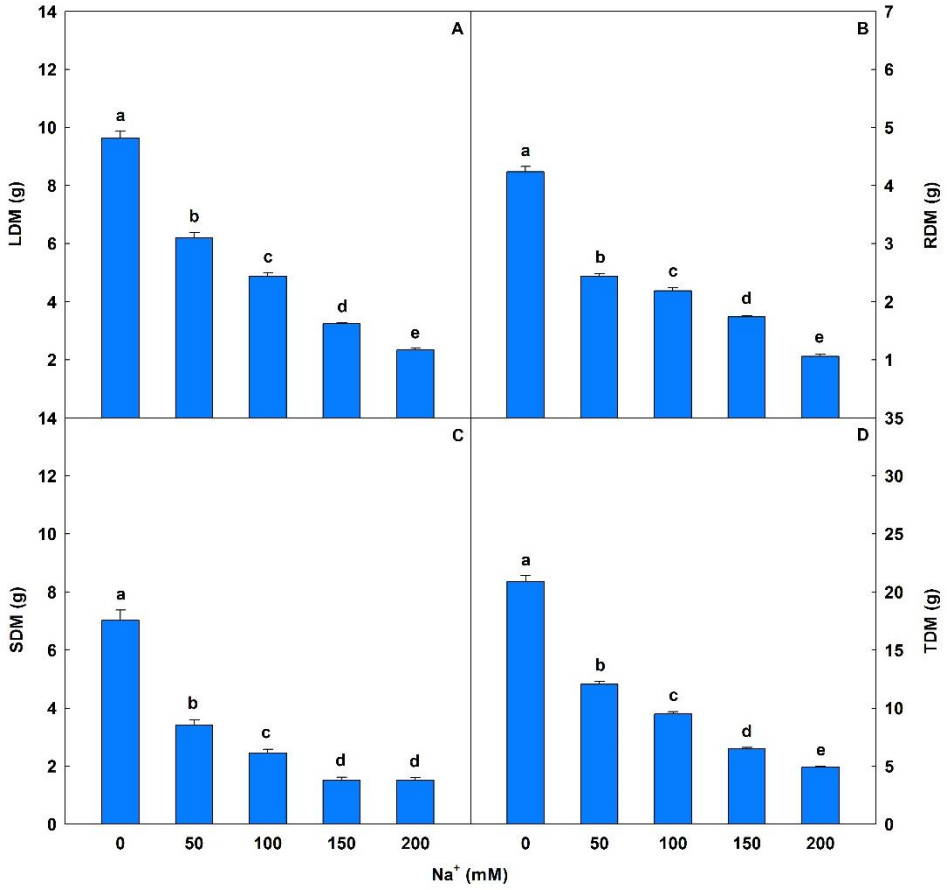

Fig. 7. Leaf dry matter (LDM), root dry matter (RDM), stem dry matter (SDM) and total dry matter (TDM) in soybean plants submitted to salt stress. Bars with different letters indicate significant differences from the Scott-Knott test (P<0.05). Bars corresponding to means from five repetitions and standard deviations.

1005

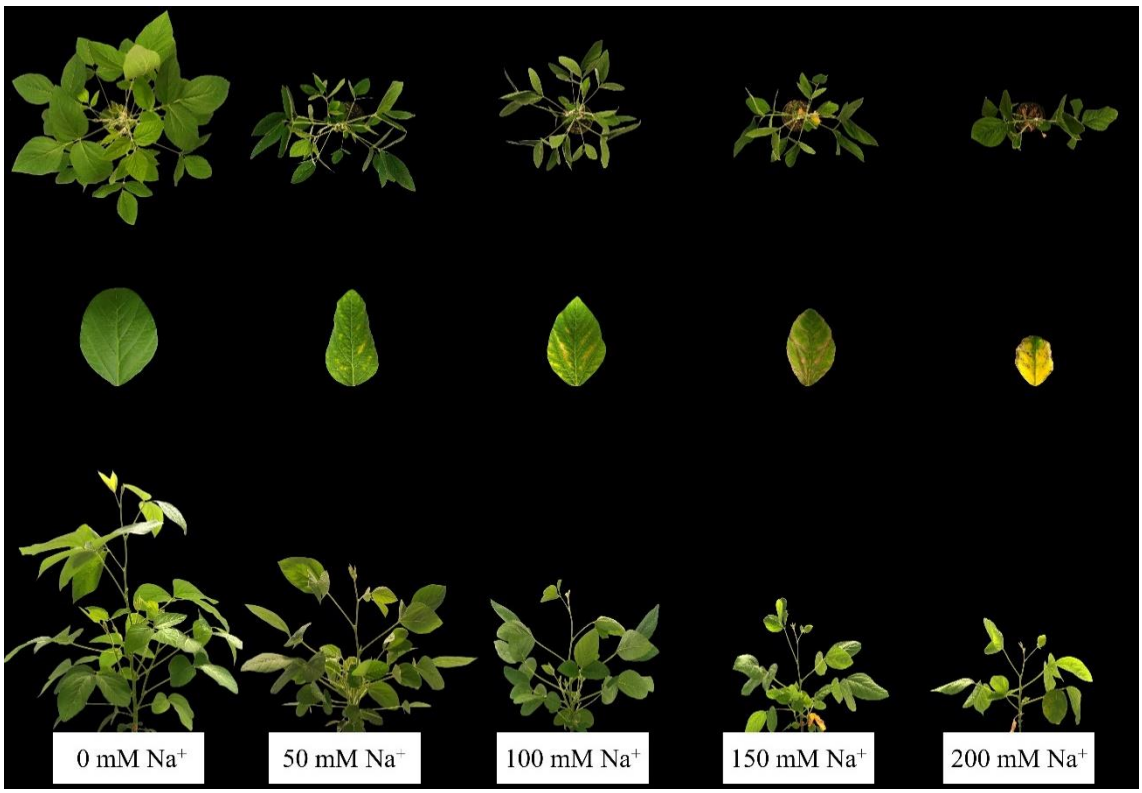

1006

1007 Fig. 8. Morphological modifications in soybean plants submitted to salt stress.

Tables

Table 1. Na and K contents and K^+/Na^+ ratio in soybean plants submitted to salt stress.

Na^+ (mM)	Na^+ in leaf (mg g DM^{-1})	K^+ in leaf (mg g DM^{-1})	K^+/Na^+ in leaf
0	0.03 ± 0.01d	8.62 ± 0.61a	1045.37 ± 84.34a
50	0.18 ± 0.01d	6.83 ± 0.30b	166.72 ± 7.45b
100	2.30 ± 0.11c	5.46 ± 0.21b	12.49 ± 0.59c
150	11.76 ± 0.20b	6.55 ± 0.14c	2.23 ± 0.06c
200	27.82 ± 0.66a	6.70 ± 0.16d	0.80 ± 0.01c

Na^+ = Sodium; K^+ = Potassium; K^+/Na^+ = Potassium and sodium ratio. Columns with different letters indicate significant differences from the Scott-Knott test ($P<0.05$). Values described corresponding to means from five repetitions and standard deviations.

Table 2. Nutrient contents in soybean plants submitted to salt stress.

Na^+ (mM)	Ca (mg g DM^{-1})	Mg (mg g DM^{-1})	S (mg g DM^{-1})	Fe (µg g DM^{-1})	Mn (µg g DM^{-1})	Cu (µg g DM^{-1})
0	18.54 ± 0.83a	4.79 ± 0.26a	2.93 ± 0.15a	108.16 ± 5.52a	66.21 ± 1.51a	2.52 ± 0.03a
50	11.55 ± 0.27b	3.82 ± 0.10b	2.53 ± 0.09b	87.65 ± 3.74b	59.47 ± 1.04b	2.19 ± 0.04b
100	8.61 ± 0.42c	3.35 ± 0.13c	2.42 ± 0.05b	79.00 ± 2.40c	57.71 ± 0.94c	2.05 ± 0.05c
150	7.37 ± 0.20d	3.11 ± 0.16c	2.21 ± 0.08c	74.37 ± 1.84d	56.00 ± 1.75c	1.97 ± 0.05d
200	6.80 ± 0.09d	2.82 ± 0.25d	2.15 ± 0.07c	65.11 ± 1.72e	47.38 ± 1.34d	1.59 ± 0.04e

Ca = Calcium; Mg = Magnesium; S = Sulphur; Fe = Iron; Mn = Manganese; Cu = Copper. Columns with different letters indicate significant differences from the Scott-Knott test ($P<0.05$). Values described corresponding to means from five repetitions and standard deviations.

Table 3. Chlorophyll fluorescence in soybean plants submitted to salt stress.

Na^+ (mM)	Φ_{PSII}	q_P	NPQ	ETR (µmol m^{-2} s^{-1})	EXC (µmol m^{-2} s^{-1})	ETR/P_N
0	0.39 ± 0.02a	0.60 ± 0.02a	0.80 ± 0.04d	57.8 ± 3.1a	0.50 ± 0.02d	3.05 ± 0.18d
50	0.34 ± 0.02b	0.59 ± 0.04a	1.05 ± 0.07c	50.6 ± 3.2b	0.54 ± 0.04c	4.30 ± 0.45d
100	0.29 ± 0.02c	0.55 ± 0.01b	1.22 ± 0.03b	42.4 ± 2.6c	0.59 ± 0.02b	11.04 ± 0.87c
150	0.26 ± 0.02d	0.53 ± 0.02b	1.31 ± 0.07b	38.6 ± 2.6d	0.60 ± 0.02b	47.87 ± 2.68a
200	0.15 ± 0.01e	0.42 ± 0.01c	1.92 ± 0.12a	21.7 ± 1.6e	0.76 ± 0.02a	29.84 ± 2.17b

Φ_{PSII} = Effective quantum yield of PSII photochemistry; q_P = Photochemical quenching coefficient; NPQ = Nonphotochemical quenching; ETR = Electron transport rate; EXC = Relative energy excess at the PSII level; ETR/P_N = Ratio between the electron transport rate and net photosynthetic rate. Columns with different letters indicate significant differences from the Scott-Knott test (P<0.05).Values described corresponding to means from five repetitions and standard deviations.

Table 4. Gas exchange in soybean plants submitted to salt stress.

Na^+ (mM)	P_N (µmol m^{-2} s^{-1})	E (mmol m^{-2} s^{-1})	g_s (mol m^{-2} s^{-1})	C_i (µmol mol^{-1})	WUE (µmol $mmol^{-1}$)	P_N/C_i (µmol m^{-2} s^{-1} Pa^{-1})
0	19.01 ± 0.93a	2.69 ± 0.16a	0.344 ± 0.013a	243 ± 5c	7.09 ± 0.68a	0.078 ± 0.005a
50	11.81 ± 0.59b	1.82 ± 0.04b	0.166 ± 0.011b	249 ± 7c	6.50 ± 0.42b	0.048 ± 0.003b
100	3.84 ± 0.11c	1.01 ± 0.09c	0.066 ± 0.005c	317 ± 11b	3.81 ± 0.28c	0.012 ± 0.001c
150	0.81 ± 0.05d	0.96 ± 0.08c	0.056 ± 0.005d	362 ± 14a	0.85 ± 0.08d	0.002 ± 0.001d
200	0.73 ± 0.05d	0.94 ± 0.06c	0.052 ± 0.004d	376 ± 11a	0.78 ± 0.06d	0.002 ± 0.001d

P_N = Net photosynthetic rate; E = Transpiration rate; g_s = Stomatal conductance; C_i = Intercellular CO_2 concentration; WUE = Water-use efficiency; P_N/C_i = Carboxylation instantaneous efficiency. Columns with different letters indicate significant differences from the Scott-Knott test (P<0.05).Values described corresponding to means from five repetitions and standard deviations.

Table 5. Stomatal and trichome characteristics in soybean plants submitted to salt stress.

Na^+ (mM)	SD (stomata per mm^2)	PDS (µm)	EDS (µm)	SF	SI (%)	TD (trichome per mm^2)	TS (µm)
Adaxial face							
0	81.3 ± 7.9c	13.5 ± 1.09b	17.34 ± 1.4b	0.45 ± 0.03b	6.01 ± 1.61b	15.47 ± 1.15a	799 ± 71a
50	116.9 ± 9.7a	13.7 ± 1.20b	18.12 ± 1.7b	0.52 ± 0.05a	6.85 ± 1.22a	8.23 ± 0.82b	608 ± 53b
100	96.6 ± 8.6b	15.2 ± 1.17a	22.30 ± 1.4a	0.44 ± 0.04b	8.02 ± 1.43a	8.18 ± 0.70b	524 ± 49c
150	85.1 ± 6.9c	9.9 ± 0.68c	17.01 ± 1.7b	0.38 ± 0.03c	5.91 ± 1.42b	6.25 ± 0.46c	422 ± 28d
200	66.1 ± 6.6d	8.3 ± 0.74d	14.99 ± 1.4c	0.32 ± 0.03d	5.40 ± 1.33b	5.92 ± 0.78c	341 ± 31e
Abaxial face							
0	304.9 ± 24.2b	13.8 ± 1.0b	21.6 ± 2.1b	0.51 ± 0.05b	15.64 ± 1.50b	33.57 ± 3.11a	705 ± 67a
50	376.1 ± 35.3a	14.7 ± 1.1a	22.3 ± 1.9b	0.58 ± 0.05a	18.39 ± 1.13a	15.80 ± 1.40b	621 ± 54b
100	213.5 ± 20.6c	10.1 ± 0.8c	25.3 ± 2.1a	0.41 ± 0.04c	12.96 ± 1.15c	12.83 ± 1.18c	560 ± 55c
150	193.1 ± 17.9c	9.7 ± 0.8c	23.1 ± 1.9b	0.39 ± 0.03c	11.56 ± 1.05d	10.61 ± 0.92d	553 ± 51c
200	106.7 ± 8.6d	8.4 ± 0.7d	13.6 ± 1.1c	0.32 ± 0.03d	7.65 ± 0.70e	5.27 ± 0.39e	314 ± 30d

SD = Stomatal density; PDS = Polar diameter of the stomata; EDS = Equatorial diameter of the stomata; SF = Stomatal functionality; SI = Stomatal index; TD = Trichome density; TS = Trichome size. Columns with different letters indicate significant differences from the Scott-Knott test ($P<0.05$).Values described corresponding to means from five repetitions and standard deviations.

Table 6. Epicuticular wax load and leaf anatomy in soybean plants submitted to salt stress.

Na^+ (mM)	EWL (mg cm^{-2})	LXT (µm)	LMD (µm)	LPT (µm)	ETAd (µm)	ETAb (µm)	PPT (µm)	SPT (µm)
0	7.09 ± 0.41b	142.2 ± 4.5c	32.6 ± 3.1a	54.0 ± 4.9b	10.57 ± 0.64b	10.17 ± 0.65b	53.7 ± 4.9c	45.8 ± 2.4b
50	7.97 ± 0.42a	161.7 ± 9.3b	33.9 ± 2.5a	72.9 ± 3.2a	11.63 ± 1.20b	14.03 ± 1.01a	60.4 ± 5.6b	46.0 ± 4.5b
100	5.59 ± 0.53c	182.2 ± 3.9a	34.7 ± 3.4a	53.2 ± 3.1b	17.12 ± 1.60a	14.81 ± 1.37a	82.9 ± 4.8a	71.9 ± 4.1a
150	4.92 ± 0.39d	135.7 ±13.3c	32.3 ± 2.0a	48.9 ± 3.0c	10.32 ± 0.59b	10.95 ± 0.60b	61.8 ± 2.0b	45.1 ± 3.1b
200	4.57 ± 0.35d	129.3 ± 12.9c	27.0 ± 2.0b	47.3 ± 3.9c	9.65 ± 0.87b	9.86 ± 0.63b	60.9 ± 2.3b	38.3 ± 2.7c

EWL = Epicuticular wax load; LXT = Leaf metaxylem thickness; LMD = Leaf metaxylem diameter; LPT = Leaf phoelm thickness; ETAd = Epidermis thickness from adaxial leaf side; ETAb = Epidermis thickness from abaxial leaf side; PPT = Palisade parenchyma thickness; SPT = Spongy parenchyma thickness. Columns with different letters indicate significant differences from the Scott-Knott test ($P<0.05$). Values described corresponding to means from five repetitions and standard deviations.

Table 7. Photosynthetic pigments in soybean plants submitted to salt stress.

Na^+ (mM)	Chl *a* (mg g^{-1} FM)	Chl *b* (mg g^{-1} FM)	Total Chl (mg g^{-1} FM)	Car (mg g^{-1} FM)	Ratio Chl *a*/Chl *b*	Ratio Total Chl/Car
0	12.27 ± 0.67a	6.67 ± 0.07a	18.94 ± 0.74a	1.05 ± 0.04a	1.44 ± 0.08b	18.08 ± 1.32c
50	10.50 ± 0.89b	5.49 ± 0.41b	15.98 ± 0.86b	0.83 ± 0.03b	1.93 ± 0.26b	19.28 ± 1.05c
100	10.42 ± 0.19b	5.31 ± 0.71b	15.73 ± 0.69b	0.77 ± 0.04c	2.00 ± 0.32b	20.58 ± 1.70c
150	9.22 ± 0.31c	2.49 ± 0.31c	11.71 ± 0.59c	0.49 ± 0.03d	3.74 ± 0.40a	24.13 ± 1.68b
200	8.25 ± 0.12d	2.07 ± 0.07c	10.32 ± 0.09d	0.31 ± 0.02e	3.98 ± 0.18a	33.13 ± 2.39a

Chl *a* = Chlorophyll *a*; Chl*b* = Chlorophyll *b*; Total chl = Total chlorophyll; Car = Carotenoids. Columns with different letters indicate significant differences from the Scott-Knott test ($P<0.05$).Values described corresponding to means from five repetitions and standard deviations.

GENERAL CONCLUSIONS

This research showed that soybean plants subjected to progressive salt stress exhibited anatomical modifications to minimize the deleterious effects associated with Na+. For all the root regions studied, increases in the epidermis and endodermis revealed the protective roles of these structures in plants subjected to 100 mM Na^+, reducing the Na^+ influx and the formation of lysogenic aerenchyma and increasing the salinity. In addition, dead cells are replaced by air spaces, thus minimizing the uptake of this toxic ion. Regarding the stems, there were increases in the cortex and pith in the first internode under concentrations of 100 mM Na^+, these being anatomical responses aiming to alleviate damage and oxidative stress generated by the salt in meristematic regions. Finally, all the root and stem regions analysed in the soybean plants subjected to concentrations of 50–200 mM Na^+ avoid cavitation and loss of function associated with vessel elements reducing the metaxylem, and this modification maximizes the impermeability of this tissue and prevents ionic flux due to increased cell wall thickness. Relative to leaves, has shown that progressive salt stress interferes negatively in K^+/Na^+ homeostasis, nutritional content, photosynthetic apparatus and gas exchange, also increases oxidative damage and to some extent induces the antioxidant system and impairs photosynthetic pigments. On the other hand, salinity impacts promote leaf anatomical modifications to minimize the deleterious effects linked to Na^+. Effects such as the increase of epicuticular wax under saline concentrations of 50 mM Na^+ favor a lipophilic protection that avoids the loss of water by perspiration and the direct incidence of solar radiation on epidermal cells. Additionally, the improvements observed in stomata quantity, in their most elliptical shape, as well as the increase of epidermis thickness, up to 100 mM Na^+, evidences a strategy for the efficient use of water.